

Comparison between Hydroxyapatite-Alginate and Whitlockite-Alginate Nano composites as Drug delivery matrix for sustained release of Ciprofloxacin



By

Alishba Arshad

(Registration No: 00000327858)

Department of Materials Engineering

School of Chemical and Materials Engineering

National University of Sciences & Technology (NUST)

Islamabad, Pakistan

(2024)

Comparison between Hydroxyapatite-Alginate and Whitlockite-Alginate Nano composites as Drug delivery matrix for sustained release of Ciprofloxacin



By

Alishba Arshad

(Registration No: 00000327858)

A thesis submitted to the National University of Sciences and Technology, Islamabad,

in partial fulfillment of the requirements for the degree of

Master of Science in
Nanoscience and Engineering

Supervisor: Dr. Zakir Hussain

School of Chemical and Materials Engineering

National University of Sciences & Technology (NUST)

Islamabad, Pakistan

(2024)

THESIS ACCEPTANCE CERTIFICATE



THESIS ACCEPTANCE CERTIFICATE

Certified that final copy of MS thesis written by Ms Alishba Arshad (Registration No 00000327858), of School of Chemical & Materials Engineering (SCME) has been vetted by undersigned, found complete in all respects as per NUST Statues/Regulations, is free of plagiarism, errors, and mistakes and is accepted as partial fulfillment for award of MS degree. It is further certified that necessary amendments as pointed out by GEC members of the scholar have also been incorporated in the said thesis.

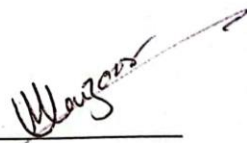
Signature: 

Name of Supervisor: Dr Zakir Hussain

Date: 8/7/2024

Signature (HOD): 

Date: 8/7/24

Signature (Dean/Principal): 

Date: 8/7/24

TH - 1



Form TH-1

(Must be type written)

National University of Sciences & Technology (NUST)

MASTER'S THESIS WORK

Formulation of Guidance and Examination Committee (GEC)

Name: Alishba Arshad

NUST Regn No: 00000327858

Department: Materials Engineering

Specialization: Nanoscience Engineering

Credit Hour Completed: 18 / 24

CGPA: 3.50 / 3.44

Course Work Completed

S/No	Code	Title	Core/Elective	CH	Grade
1	RM-898	Research Methodology	Additional	2	Q
2	NSE-813	Essentials of Nanoscience and Engineering	Core	3	B+
3	MSE-854	Characterization Of Materials	Elective	3	B+
4	NSE-845	Nanolithography And Device Fabrication	Core	3	A
5	MSE-856	Nano Material and Processing	Core	3	B
6	MSE-872	Composite Materials	Elective	3	B+
7	NSE-812	Environmental Nanotechnology	Elective	3	B+
8	MSE-879	Functional Nanomaterials for Renewable Energy		3	B
9	NSE-961	Surface coatings & Thin Films		3	B+

Date: 24th Sep 2021

Student's Signature: Alishba

Thesis Committee

- Name: Dr. Zakir Hussain (Supervisor)
Department: Materials Engineering
- Name: Dr. Usman Liaqat (Co-Supervisor)
Department: Materials Engineering
- Name: Dr. Muhammad Aftab Akram (Member)
Department: Materials Engineering
- Name: Dr. Muhammad Bilal Khan Niazi (Member)
Department: Chemical Engineering

Signature: [Signature]
Signature: [Signature]
Signature: [Signature]
Signature: [Signature]

Date: 30/9/2021

Signature of Head of Department: [Signature]

APPROVAL

Date: 8.10.2021

Dean/Principal: [Signature]

Distribution

1x copy to Exam Branch, Main Office NUST

1x copy to PGP Dte, Main Office NUST

1x copy to Exam branch, respective institute

School of Chemical and Materials Engineering (SCME) Sector H-12, Islamabad

TH – 4



National University of Sciences & Technology (NUST)

FORM TH-4

MASTER'S THESIS WORK

We hereby recommend that the dissertation prepared under our supervision by

Regn No & Name: 0000327858 Alishba Arshad

Title: Comparison between Hydroxyapatite-Alginate and Whitlockite-Alginate Nanocomposite Beads as Drug Delivery Matrix for Sustained Release of Ciprofloxacin.

Presented on: 13 Jun 2024 at: 1500 hrs in SCME Seminar Hall

Be accepted in partial fulfillment of the requirements for the award of Masters of Science degree in **Nanoscience & Engineering**.

Guidance & Examination Committee Members

Name: Dr M. Aftab Akram

Signature: [Signature]

Name: Dr M. Bilal Khan Niazi

Signature: [Signature]

Name: Dr Usman Liaqat (Co-Supervisor)

Signature: [Signature]

Supervisor's Name: Dr Zakir Hussain

Signature: [Signature]

Dated: 13/6/2024

[Signature]
Head of Department
Date 14/6/24

[Signature]
Dean/Principal
Date 14/6/24

School of Chemical & Materials Engineering (SCME)

AUTHOR'S DECLARATION

I Alishba Arshad hereby state that my MS thesis titled “Comparison between Hydroxyapatite-Alginate and Whitlockite-Alginate Nano composites as Drug delivery matrix for sustained release of Ciprofloxacin” is my own work and has not been submitted previously by me for taking any degree from National University of Sciences and Technology, Islamabad or anywhere else in the country/ world.

At any time if my statement is found to be incorrect even after I graduate, the university has the right to withdraw my MS degree.

Name of Student: Alishba Arshad

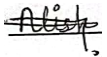
Date: 18 July 2024

PLAGIARISM UNDERTAKING

I solemnly declare that research work presented in the thesis titled “Comparison between Hydroxyapatite-Alginate and Whitlockite-Alginate Nano composites as Drug delivery matrix for sustained release of Ciprofloxacin” is solely my research work with no significant contribution from any other person. Small contribution/ help wherever taken has been duly acknowledged and that complete thesis has been written by me.

I understand the zero-tolerance policy of the HEC and National University of Sciences and Technology (NUST), Islamabad towards plagiarism. Therefore, I as an author of the above titled thesis declare that no portion of my thesis has been plagiarized and any material used as reference is properly referred/cited.

I undertake that if I am found guilty of any formal plagiarism in the above titled thesis even after award of MS degree, the University reserves the rights to withdraw/revoke my MS degree and that HEC and NUST, Islamabad has the right to publish my name on the HEC/University website on which names of students are placed who submitted plagiarized thesis.

Student Signature: 

Name: Alishba Arshad

DEDICATION

“I dedicate this thesis to my daughter.”

ACKNOWLEDGEMENTS

All admiration to Allah Almighty who is all omnipotent and Regulator of the whole Universe. He is the only One, who bestows and gives the power to us to think, utilize our expertise in knowledge in achieving remarkable solutions for mankind in every field. Therefore, I express my greatest obligations to Almighty Allah the universal and the architect of all universe, who has gifted us a brain, intelligence and unhinged nature creation of knowledge and physique to achieve our desired work in the form of this project report.

I would like to express my gratefulness to my very nice and respected supervisor Dr. Zakir Hussain for their clear and patient guidance that directed me to fulfill my research project and this thesis.

I acknowledge the support provided by the Materials Engineering department of SCME, for providing me a platform to perform my experiments and using my skills in research work.

I acknowledge the financial aid and technical assistance provided by our department, SCME, during my research experience and made this project work memorable forever.

Alishba Arshad

TABLE OF CONTENTS

ACKNOWLEDGEMENTS	IX
TABLE OF CONTENTS	X
LIST OF TABLES	XII
LIST OF FIGURES	XIII
LIST OF SYMBOLS, ABBREVIATIONS AND ACRONYMS	XV
ABSTRACT	XVI
CHAPTER 1: INTRODUCTION	1
1.1 Nano science and Nanotechnology	1
CHAPTER 2: LITERATURE REVIEW	4
2.1 Bio-Ceramics	4
2.1.1 Hydroxyapatite (HA)	5
2.1.2 Whitlockite	7
2.2 Sodium Alginate	9
2.2.1 (G-(O-CH ₂ -CH ₂) n-M) m	9
2.3 Ciprofloxacin (CPX)	11
2.4 Application in Biomedical Engineering	12
2.4.1 Drug Delivery	13
2.4.2 Scaffolds	14
2.4.3 Coating of implants	15
2.5 What are Nano composites?	16
2.5.1 History of Biomedical nanocomposites	16
2.5.2 Synthesis of biomedical application of nanocomposites with up conversion nanoparticles	17
2.6 Application of Bioactive nanocomposites in Bone tissue regeneration	18
2.6.1 Bioactive nanocomposite scaffolds	18
2.6.2 Nanocomposite hydrogels for biomedical applications	19
2.6.3 Polymeric nanocomposite beads for Drug Delivery application	20
2.6.4 Alginate composite systems as sustained drug delivery carriers	20
2.7 Hydroxyapatite-Alginate based Nanocomposite beads for drug delivery application	21
2.8 Whitlockite nanocomposites for biomedical applications	23
2.9 Objectives	24
CHAPTER 3: MATERIALS AND METHODS	26
3.1 Synthesis and characterization of Hydroxyapatite nanoparticles	26
3.1.1 Drug loading	27

3.1.2	Preparation of Ciprofloxacin loaded Hydroxyapatite-Alginate composite	28
3.1.3	Drug Release	28
3.2	Preparation of Whitlockite based Nanocomposite beads	29
3.2.1	Synthesis and characterization of Whitlockite nanoparticles	29
3.2.2	Drug loading	30
3.2.3	Preparation of Ciprofloxacin loaded Whitlockite-Alginate composite	30
3.2.4	Drug Release	31
CHAPTER 4:	CHARACTERIZATION TECHNIQUES	33
4.1	Scanning Electron Microscopy	33
4.2	X-ray diffraction (XRD)	35
4.3	Fourier Transform Infrared (FT-IR) Spectroscopy	37
4.4	Raman Analysis	39
4.5	UV-vis Spectroscopy	40
4.6	Physical Characterization of Nanocomposite Beads	43
4.6.1	Swelling Test	43
CHAPTER 5:	RESULTS AND DISCUSSION	44
5.1	Fourier Transformation – IR (FTIR) Analysis	44
5.1.1	FT-IR of Hydroxyapatite-Drug powder	44
5.1.2	FT-IR of Hydroxyapatite-Alginate Nano composite beads loaded with Drug	47
5.1.3	FT-IR of Whitlockite-Drug powder	47
5.1.4	FT-IR of Whitlockite-Alginate Nano composite beads loaded with Drug	50
5.2	X-ray Diffraction (XRD) Analysis	50
5.2.1	XRD Analysis of Hydroxyapatite-Drug Powder	51
5.2.2	XRD Analysis of Hydroxyapatite-Alginate nanocomposite beads loaded with Drug	52
5.2.3	XRD Analysis of Whitlockite-Drug Powder	54
5.2.4	XRD of Whitlockite-Alginate nanocomposite beads loaded with Drug	55
5.3	Raman Analysis	56
5.3.1	Raman Analysis of Hydroxyapatite-Drug Powder	56
5.3.2	Raman Analysis of Whitlockite-Drug Powder	57
5.4	Scanning Electron Microscopy (SEM) of Nano composite Beads	58
5.4.1	SEM Analysis of Hydroxyapatite-Alginate beads loaded with drug	58
5.4.2	SEM Analysis of Whitlockite-Alginate beads loaded with drug	59
5.5	Swelling behavior of HA-Alginate beads loaded with drug	61
5.6	Swelling behavior of WH-Alginate beads loaded with drug	62
5.7	Drug Delivery Analysis of HA-Alginate beads loaded with drug	64
5.8	Drug Delivery Analysis of WH-Alginate beads loaded with drug	66
CHAPTER 6:	CONCLUSIONS AND FUTURE RECOMMENDATION	68
6.1	Conclusion	68
6.2	Future Work and Recommendation	69
REFERENCES		70

LIST OF TABLES

Table 3.1: Drug loading in percentage for Hydroxyapatite-Alginate composite with different drug concentrations.	28
Table 3.2: Drug loading in percentage for Whitlockite- Alginate composite with different drug concentrations.	31

LIST OF FIGURES

Figure 1.1: Role of Nanotechnology in Drug.	3
Figure 2.1: Classification of Nanocomposites	5
Figure 2.2: Structure of Nano hydroxyapatite.	6
Figure 2.3: Synergistic interplay between two bone minerals, Hydroxyapatite and Whitlockite nanoparticles [15].....	7
Figure 2.4: Bone Whitlockite [17].....	8
Figure 2.5: Structure of Sodium Alginate.....	11
Figure 2.6: Structure of Ciprofloxacin.....	12
Figure 2.7: Applications of Nanobiocomposites [28].....	13
Figure 2.8: Drug Delivery by Nano composites	14
Figure 2.9: Scaffolds for bone tissue regeneration	15
Figure 3.1: Schematics of Whitlockite synthesis.....	30
Figure 4.1: (a) JOEL JSM-6490LA SEM at SCME; (b) Schematics of SEM.....	35
Figure 4.2: XRD present at SCME- NUST (b) XRD basic schematics	36
Figure 4.3: Working schematics of FT-IR Spectroscopy	39
Figure 4.4: Schematics showing Raman scattering process	40
Figure 4.5: UV-vis spectrometer Optima SP-3000DB	42
Figure 5.1: FTIR spectrum of pure HA	44
Figure 5.2: (a) FT-IR of Hydroxyapatite-Drug powder with different drug ratios.....	45
Figure 5.3: FT-IR of Hydroxyapatite-Alginate Nano composite beads loaded with different Drug ratios.....	46
Figure 5.4: FTIR of PURE WH.....	48
Figure 5.5: FT-IR of Whitlockite-Drug powder with different drug ratios	48
Figure 5.6: FT-IR of Whitlockite-Alginate nanocomposite beads loaded with different drug ratios	49
Figure 5.7: XRD of pure HA	51
Figure 5.8: XRD Analysis of HA-Drug powder with different drug ratios.....	53
Figure 5.9: XRD Analysis of Hydroxyapatite-Alginate nanocomposite beads loaded with Drug.	53
Figure 5.10: XRD Analysis of WH-Drug powder with different drug ratios.....	54
Figure 5.11: XRD Analysis of HA-Alginate nanocomposite beads loaded with different drug ratios	55
Figure 5.12: Raman Analysis of Hydroxyapatite-Drug Powder with different drug ratios	56
Figure 5.13: Raman Analysis of Whitlockite-Drug powder with different drug ratios...	57
Figure 5.14: SEM analysis of HA-Alginate and WH-Alginate nanocomposite beads loaded with different drug ratios.....	60
Figure 5.15: Swelling Behaviour of HA-Alginate nanocomposite beads loaded with different drug ratios.....	62

Figure 5.16: Swelling Behaviour of WH-Alginate nanocomposite beads loaded with different drug ratios.....	63
Figure 5.17: Drug Delivery Analysis of HA-Alginate nanocomposite beads loaded with different drug ratios.....	65
Figure 5.18: Drug Delivery Analysis of WH-Alginate nanocomposite beads loaded with different drug ratios.....	66

LIST OF SYMBOLS, ABBREVIATIONS AND ACRONYMS

Abbreviation	Meaning
at%	Atomic Percent
CPX	Ciprofloxacin
DI	Distilled Water
DNA	Deoxyribose Nucleic Acid
EDX	Energy Dispersive X-ray
HA	Hydroxyapatite
JCPDS	Joint Committee on Powder Diffraction Standards
KBr	Potassium Bromide
NM	Nanomaterials
NP	Nanoparticles
PBS	Phosphate Buffer Solution
SA	Sodium Alginate
SEM	Scanning Electron Microscope
TEM	Transmission Electron Microscopy
UV-vis	Ultraviolet Visible
WH	Whitlokite
wt%	Weight Percent
XRD	X-ray Diffraction

ABSTRACT

For bone tissue engineering and bone remodelling, functional biomaterials that connect the processes of angiogenesis and osteogenesis are essential. The presence of nanoparticles in polymers results in the creation of polymeric nanocomposites, which increase the characteristics of the nanoparticles and polymer. It is feasible to enhance the osteoinductive and osteoconductive properties of the bones by utilising ceramic materials like nHA (nano-hydroxyapatite) and nWH (nano-whitlockite). According to literature the most prevalent inorganic phases in the skeletal tissues are HA and WH. Comparison between nano-hydroxyapatite (nHA) and whitlockite (nWH) nanocomposite beads for sustained release of drug ciprofloxacin for bone tissue regeneration is elucidated in this project. Morphology, crystallinity, degradation and drug release studies of composites were carefully assessed. Briefly, nHA and nWH nanoparticles were synthesized by wet chemical precipitation method and further carried out by drug loading procedures in which the drug was absorbed on to the nHA and nWH surfaces. Different compositions were made by varying the drug loading percentages. Chemical analysis of the prepared nanoparticles and composites was carried out using X-ray Diffraction (XRD), Fourier Transform infrared spectrophotometry (FTIR), and Raman Analysis. Results of composites conclude that nHA and nWH were carefully inserted into the polymer matrix and remained well intact with the alginate macromolecules. Research has been conducted on the loading and release of drugs. Prior to the composite's formation, the drug ciprofloxacin was pre-adsorbed onto the ceramic particles. Results confirmed that the nanocomposites prepared under optimum condition prolonged the release of ciprofloxacin which hold a great benefit in bone tissue engineering. Hence it was proved that both of the ceramic materials Hydroxyapatite and Whitlockite can be used to improve the efficacy of bone regeneration and could be a good candidate for bone tissue engineering.

Keywords: Nanoparticles, Nanocomposite, Hydroxyapatite, Whitlockite, Sodium alginate, Bone tissue engineering.

CHAPTER 1: INTRODUCTION

Science is more than merely the systematic study of the natural world or even a corpus of knowledge about it. Science is an approach to studying nature that produces reliable data about it and an approach to learning about it. Stated differently, science is an approach to acquiring reliable information about the natural world.

There are other ways to discover new things and learn about nature (these alternative knowledge systems and approaches will be discussed below in contrast to science), but science is the only path that results in reliable information being acquired. Physical sciences, life sciences, and earth sciences, which are the three main subfields of the comprehensive field of natural sciences, are the divisions of modern scientific study.

1.1 Nano science and Nanotechnology

Nanoscience and nanotechnology are interdisciplinary fields of science and engineering that deal with the study and handling of materials at the nanoscale. Greek word "nanos" (meaning "dwarf") is where the word "nano" originates.

In scientific terms, a nanometer (nm) is a unit of measurement that is equal to one billionth of a meter.

Nanoscience focuses on the study of properties of matter at the nanoscale, including the discovery of new phenomena and the understanding of the underlying principles that govern these behaviors.

Nanotechnology, on the other hand, is the application of this knowledge to create new materials, unique devices, and next generation systems with improved properties and functionality[1].

The unique properties of materials at the nanoscale result from the increased surface area to volume ratio and the quantum size effects that arise at this scale. These

properties make nanoscale materials ideal for a vast range of applications, including electronics, energy, biomedicine, and many others[2].

In conclusion, nanoscience and nanotechnology represent a new frontier of scientific discovery and technological advancement, with the potential to revolutionize many areas of science and technology.

Nanotechnology is an interdisciplinary field that combines different sciences together. It includes biotechnology and nanotechnology to develop biomedical devices which integrate biomolecular machinery such as Biomolecules, DNA, proteins, viral and bacterial particles and pharmaceutical ingredients into the materials of choice.

We have carried our research to make nanotechnology very useful and affordable in fields of therapeutics particularly antibiotic drugs. The bioceramics and biopolymers used also modified the biological properties of drugs and assist in healing and defense from pathogens[3].

Scientists are working actively on delivering the drugs to the targeted site using different routes so that their mode of action is increased. All the polymeric materials, metal ligands, ceramic materials are used to interact and transport drug to the site where it is required without doing any harm to other biological environment of body.

The combination of bioceramics, biopolymers and drugs enhance the process of healing and also strengthen the defense against pathogens which helps in quick bone tissue regeneration [4].

Our research has paid attention on the formation and characterization of bioceramics Hydroxyapatite nHA and Whitlockite nWH functionalized polymeric nanocomposite beads for drug delivery application. The materials that we used were easily available and affordable.

Their characterizations were carried out easily at our campus and did not require any expensive techniques.

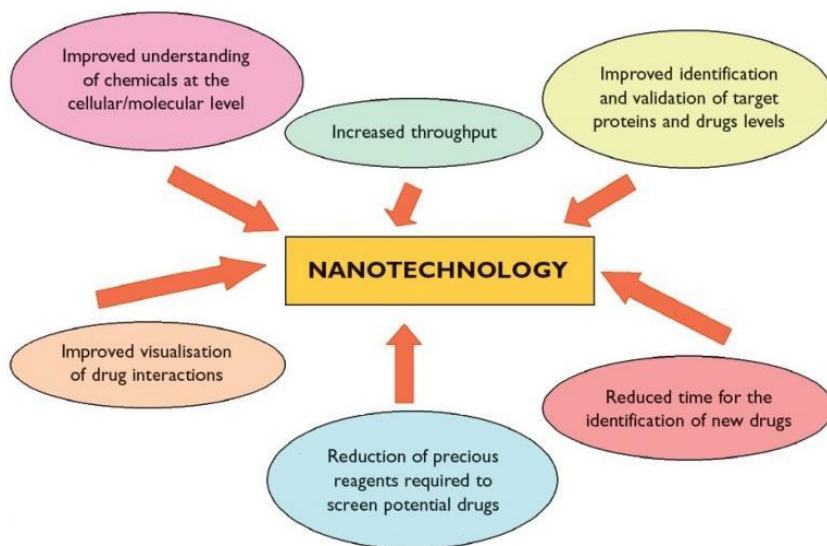


Figure 1.1: Role of Nanotechnology in Drug.

CHAPTER 2: LITERATURE REVIEW

2.1 Bio-Ceramics

Nanobioceramics refer to ceramic materials that have been engineered on a nanoscale level and are used in the field of medicine and biotechnology. These materials can have unique properties such as high biocompatibility, mechanical strength, and resistance to degradation, making them better for a variety of biomedical applications[5].

Some common types of nanobioceramics include hydroxyapatite, zirconia, and aluminosilicate. Hydroxyapatite, for example, is a bioceramic material that closely resembles the mineral composition of natural bones. Zirconia is another bio ceramic material that has been used in dental implants and has shown promise in the development of artificial joints[6].

Nanobioceramics are also being researched for their role in drug delivery systems. These materials can be designed to release drugs in a controlled manner over time, which can help improve the efficacy and safety of drug treatments. Additionally, nanobioceramics are being explored as a material for biosensors, which can be used to detect specific biomolecules and help diagnose diseases.

Nanobiocomposites are biological elements, that include proteins, DNA, or cellulose, with inorganic nanoparticles. Use of nanoparticles in nanobiocomposites provides increased mechanical, thermal, and optical properties, while the biological components add biocompatibility, biodegradability, and biological functionality[7]

For example, one type of nanobiocomposite that gained importance in this field is the combination of bioceramic nanoparticles with biopolymers, such as Sodium Alginate and starch.

This type of nanobiocomposite has potential applications in the drug delivery application, where they can be used to increase bone tissue regeneration[8]. Figure 2.1 shows the various kinds of biocomposites.

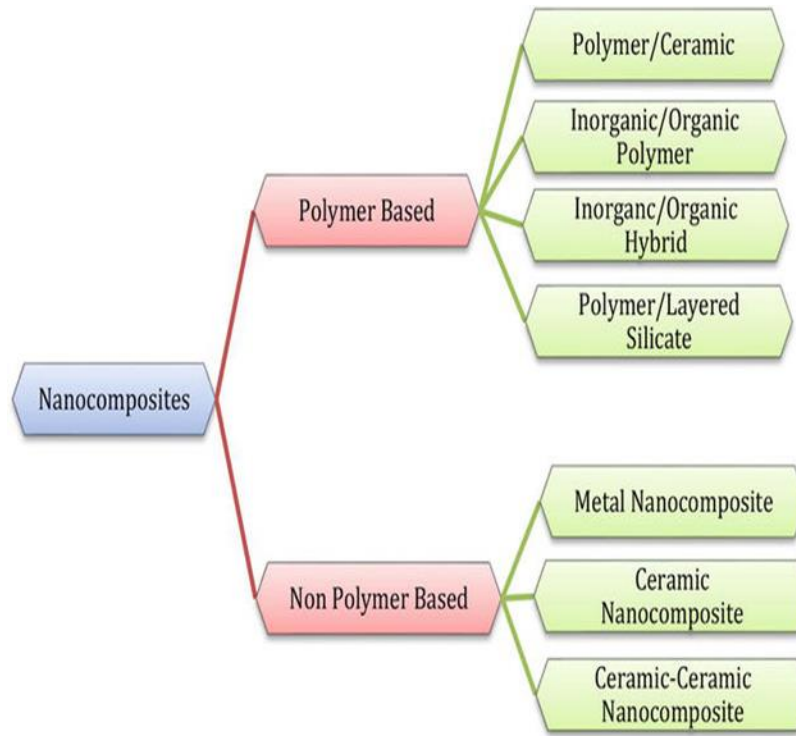


Figure 2.1: Classification of Nanocomposites

2.1.1 Hydroxyapatite (HA)

Hydroxyapatite is a synthetic form of calcium phosphate that is same as the mineral component of natural bone. Figure shows the structure of Nanohydroxyapatite powder. It is used in different medical applications, particularly in orthopedic and dental surgery[9].

Hydroxyapatite bioceramics are biocompatible and can be easily integrated into living tissues, making them an attractive material for use in implants, such as joint replacements and dental implants. Additionally, hydroxyapatite bioceramics have been observed to have a stimulating effect on bone tissue regeneration, making them useful for repairing damaged bones[10].

There are different types of hydroxyapatites bioceramics, including pure hydroxyapatite, biphasic calcium phosphate, and tricalcium phosphate. They are produced through various methods, including precipitation, sol-gel, and melting methods, and can be shaped into various forms, such as porous scaffolds, coatings, and bulk implants.

Overall, hydroxyapatite holds importance in tissue engineering, due to its good biocompatibility, osteoconductivity, and the potential to promote bone regeneration. However, further research is important to fully understand their long-term behavior in the body and optimize their clinical performance[11].

For more than six years, hydroxyapatite (HA) has been in use. In more recent times, we have filled or spaced-out bone lesions using HA composites in clinical orthopaedics. High density polyethylene wear particles are avoided with cement-fixed HA implants. Femoral plugs used in total hip replacements and HA coating on metal parts used for cementless fixation are two other uses for HA. Porous metal surfaces are made suitable for quick and effective cementless fixing; HA coating of porous metal produces better outcomes. By placing tiny HA particles between the bone and PMMA cement, we have also created a method for bioactive interfacial bone cementation[12].

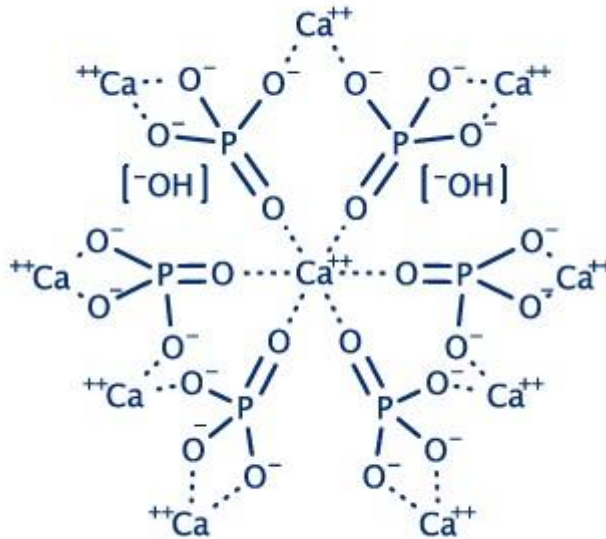


Figure 2.2: Structure of Nano hydroxyapatite.

Only calcium and phosphate ions are present in HA, hence no studies have noted any negative local or systemic toxicity. At the bone implant interface, a carbonated calcium-deficient apatite layer at the time of implant allows freshly formed bone to attach

to HA directly. Additionally, cytokines with the strength to bind and concentrate bone morphogenetic proteins (BMPs) in vivo can be delivered using HA scaffolds[13].

2.1.2 Whitlockite

Whitlockite is a mineral that belongs to the apatite group and is composed of calcium, phosphorus, and hydrogen. It is usually found in association with other minerals such as calcite, quartz, and fluorite and is typically a pale yellow to brown color. The mineral is named after American mineralogist Augustus Charles Whitlock.

Whitlockite is of interest to scientists and geologists due to its occurrence in some meteorites, and as a potential source of phosphorus, which is an essential nutrient for plants and animals. However, it is not a common mineral and is not commonly used for industrial or commercial purposes[14]

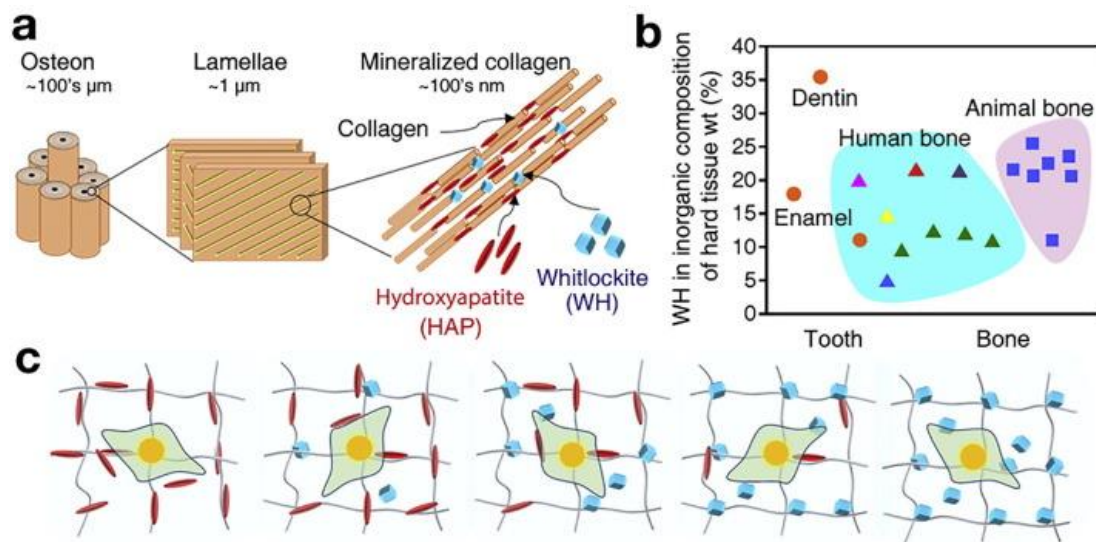


Figure 2.3: Synergistic interplay between two bone minerals, Hydroxyapatite and Whitlockite nanoparticles [15]

Whitlockite is a tricalcium phosphate with the formula $\text{Ca}_3 (\text{PO}_4)_2$. It is rhombohedral, likely scalenohedral and is a hydrothermal mineral found with whitlockite, quartz, rhodochrosite, apatite, and zeolite in granite pegmatite in the Palermo quarry, close to North Groton, New Hampshire. From a structural standpoint, Whitlockite is different

from graftonite, caryinite, fillowite, and apatite. named in honour of Herbert P. Whitlock, the American Museum of Natural History's curator of minerals and gems[15]

Whitlockite is a calcium phosphate mineral that is structurally similar to hydroxyapatite, which is the main mineral component of human bones. While hydroxyapatite is widely used in the biomedical field for bone tissue engineering and regeneration, whitlockite has not been widely used for these purposes [17].

However, recent studies have shown that whitlockite has the ability to serve as a biocompatible material for bone tissue regeneration due to its high calcium and phosphorus content, which is essential for the growth and development of bones. In addition, whitlockite has a higher mechanical strength compared to hydroxyapatite, which makes it a better material for use in load-bearing bone implants[16].

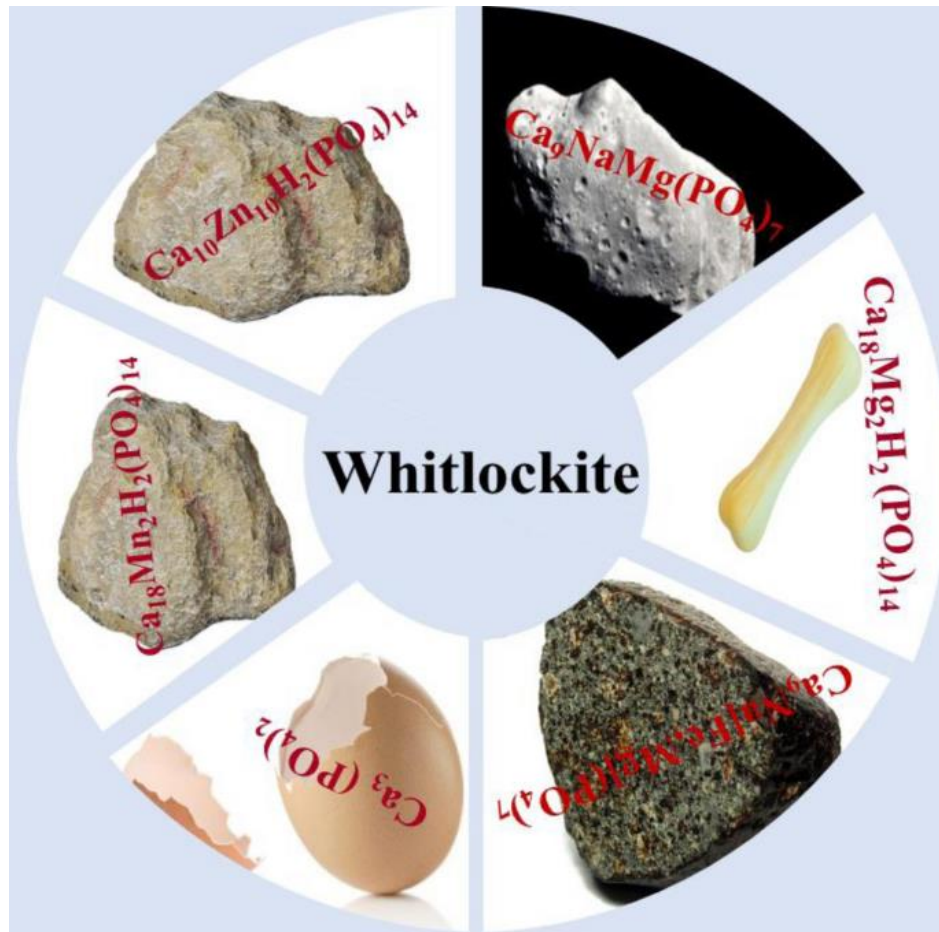


Figure 2.4: Bone Whitlockite [17]

2.2 Sodium Alginate

Sodium alginate is a linear, unbranched polysaccharide composed of β -D-mannuronic acid (M) and α -L-guluronic acid (G) units, which are linked through glycosidic bonds. The repeating unit of sodium alginate is (G-M) n , where n is the degree of polymerization and can range from several hundred to several thousand.

The chemical structure of sodium alginate can be represented as follows:



Where n and m represent the degree of polymerization and the ratio of G and M units, respectively. The "O-CH₂-CH₂" represents the sodium ion (Na⁺) that is associated with each carboxyl group in the alginate polymer, forming sodium alginate [17]. Figure shows the chemical representation of Sodium Alginate.

Sodium alginate is a polysaccharide. It is commonly used as a food thickener, emulsifier, and stabilizer, as well as in the production of soft capsules and other pharmaceutical products. Sodium alginate forms a gel-like substance when it reacts with calcium ions, making it useful in a various application. It is also used in the textile industry as a printing thickener, and in the cosmetic industry as an ingredient in various skin care and beauty products. Overall, sodium alginate has unique properties and has potential for use in many different industries[18].

Here are some of the ways in which Sodium Alginate is used in the biomedical field[19]

Wound Healing: Sodium Alginate has wound-healing properties, and when applied topically as a gel, it can help to promote the growth of new tissue and reduce inflammation.

Drug Delivery: Sodium Alginate can be used as a matrix to develop controlled-release drug delivery systems. The polymer can form hydrogels in the presence of divalent cations, which can be used to entrap and release drugs in a controlled manner.

Tissue Engineering: Sodium Alginate can be used to create scaffolds for tissue engineering. The scaffolds can provide a supportive environment for the growth of cells and the development of new tissue.

Dental Impression Material: Sodium Alginate is used as a dental impression material, where it is mixed with water to form a paste that is applied to the teeth. When the paste sets, it forms a mold of the teeth, which is then used to make dental prosthetics.

Antacid: Sodium Alginate has been shown to act as an antacid by forming a gel-like substance when it comes into contact with stomach acid. This gel can help to reduce the symptoms of heartburn and acid reflux by neutralizing excess acid in the stomach.

Overall, Sodium Alginate is a versatile polymer that has a range of biomedical applications, and its use is expected to continue to grow as researchers continue to explore its potential. Alginates are naturally occurring polymers that exhibit low toxicity, great gelling and thickening capabilities, strong biocompatibility and biodegradability, low production costs, and good availability.

Although sodium alginate is a well-known polymer, it is still often used as a pharmaceutical excipient, and the research findings that have been provided suggest that there are still areas of research that can be investigated and led to innovation in drug delivery systems[20].

Bone tissue engineering is a cutting-edge method for healing shattered and defective bone tissues. The number of persons suffering from bone problems is gradually rising globally. Sodium alginate (SA), the sodium salt of alginate, has a number of special qualities, including biodegradability, biocompatibility, gelation, and non-toxicity. Because of these characteristics, SA is a well-known and promising material in tissue engineering, medication delivery, and wound healing.

The biopolymer is appropriate for use in biomedical engineering since it can be converted into 3D porous scaffold materials. These compounds have been utilized to facilitate bone regeneration, heal shattered bones, and promote desirable cell proliferation[21].

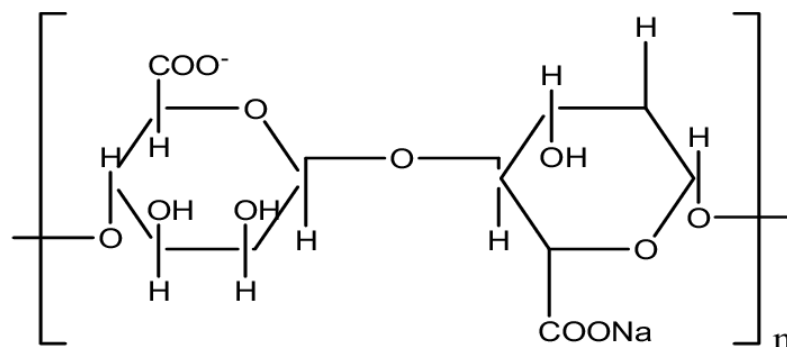


Figure 2.5: Structure of Sodium Alginate

2.3 Ciprofloxacin (CPX)

Ciprofloxacin is a fluoroquinolone antibiotic that has the chemical formula $C_{17}H_{18}FN_3O_3$. It has a cyclic structure consisting of a central ring system comprised of an aromatic ring and a quinolone ring, as well as various functional groups including a fluorine atom, a carboxyl group, a nitrogen atom, and an amine group. The molecular weight of ciprofloxacin is 331.3 g/mol[22].

Ciprofloxacin is a type of antibiotic in the fluoroquinolone family. It is used to treat a vast range of bacterial infections, like skin and respiratory infections, urinary tract infections, and some sexually transmitted infections. Ciprofloxacin works by preventing bacteria from reproducing and repairing themselves, which ultimately leads to the decay of the bacteria.

It is important to note that ciprofloxacin should be used to cure various bacterial infections and should not be used to treat viral infections, such as the common cold or flu, as it will not be effective. It is also necessary to take ciprofloxacin exactly as prescribed by a healthcare provider and to finish the entire course of treatment, even if symptoms improve, to help prevent the development of antibiotic-resistant bacteria[23].

Common side effects of ciprofloxacin can include nausea, diarrhea, and headache. More serious side effects, although rare, can include tendon damage, nerve problems and changes in heart rhythm. It is necessary to consult to a healthcare provider about the potential benefits and risks of taking ciprofloxacin[24].

Also, as we know there are improvements seen in antibiotic therapy, bone infections still significantly increase the risk of morbidity due to lingering damage and persistent recurrent infections. The surgical removal of dead bone tissue, frequent irrigation of the lesion, and prolonged systemic administration of high doses of antibiotics are all necessary for the treatment of chronic osteomyelitis.[25]

It is currently a recognized systemic therapeutic strategy to treat osteomyelitis using fluoroquinolones. The most used fluoroquinolone drug for bacterial bone infections is ciprofloxacin (CFX).

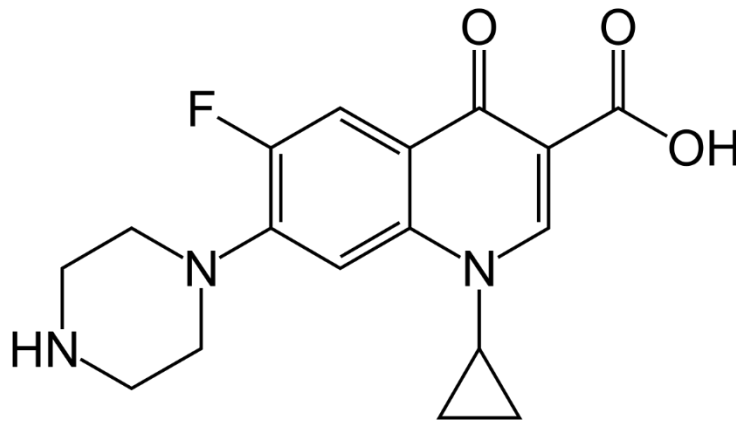


Figure 2.6: Structure of Ciprofloxacin

2.4 Application in Biomedical Engineering

Bio ceramics and Bionanocomposites play a significant part in biomedical engineering because of their unique properties, such as biocompatibility, bioactivity, mechanical strength, and durability.

These properties make Bio ceramics and Bionanocomposites suitable for use in various medical applications, such as shown in Figure 2.7.

- Dental restorations: Bioceramics, such as alumina and zirconia, are commonly used for dental crowns, bridges, and implants because of their high strength, durability, and biocompatibility with oral tissues.

- Joint replacements: Bioceramics, such as alumina and zirconia, are also used in joint replacements, such as hip and knee implants, due to their biocompatibility, toughness, and wear resistance.
- Tissue engineering: Bioceramics can also be used as scaffolds in tissue engineering, supplying a framework that encourages cell proliferation and tissue regeneration.
- Drug delivery: Bioceramics can be functionalized with drugs and used as drug delivery devices, providing sustained release of therapeutic agents to the target site.
- Cancer treatment: Bio ceramics, such as hydroxyapatite, can also be used in cancer treatment, either as a carrier for chemotherapy drugs or as a radiotherapy enhancer.

Overall, bio ceramics play a crucial role in biomedical engineering and offer promising solutions for wide range of medical applications.

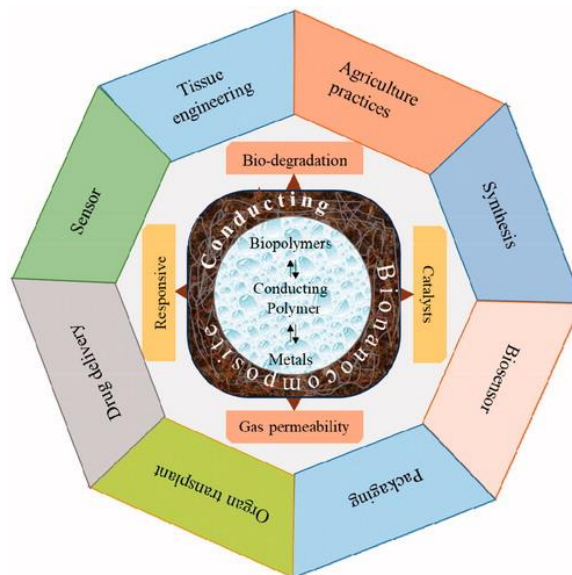


Figure 2.7: Applications of Nanobiocomposites [28]

2.4.1 Drug Delivery

The developed nanocomposite beads must be able to physically or chemically load a drug, hold the drug till it reaches the precise target site, degrade slowly, and transport the

drug in a sustained manner over period of time in order to be employed as a drug carrier[26].

Calcium phosphates (CaPs) successfully satisfy all requirements, making them interesting materials for applications involving drug delivery. Due to their remarkable bioactivity and chemical similarities to bone mineral, CaPs are frequently employed in bone and tissue engineering for hard tissues like teeth or bone replacement, augmentation, or regeneration. The drug delivery by nanocomposites also shown in Figure 9.

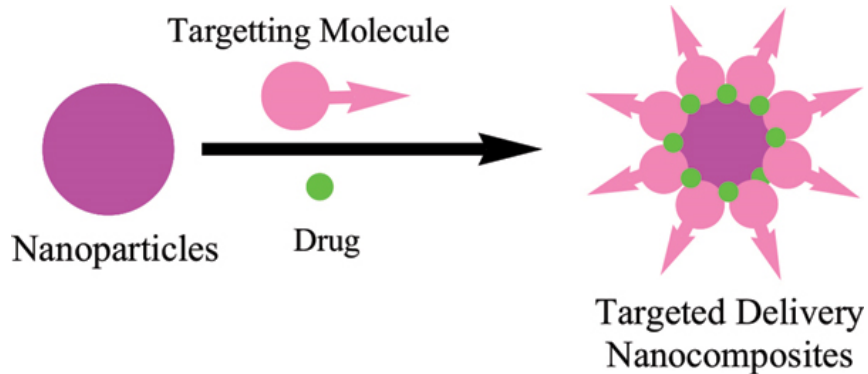


Figure 2.8: Drug Delivery by Nano composites

2.4.2 Scaffolds

Nanocomposite scaffolds are three-dimensional structures made from a combination of different materials at the nanoscale level. These materials can include biodegradable polymers like Sodium alginate, bioceramics like Hydroxyapatite and Whitlockite nanoparticles.

The aim of using nanocomposites in scaffolds is to improve the characteristics of the scaffold such as mechanical strength, biocompatibility, and biodegradability, which are crucial elements for achievement of tissue engineering[27].

Nanocomposite scaffolds are used in tissue engineering applications, including bone regeneration, skin tissue engineering, and cartilage repair. The nanoscale components of the scaffold like Hydroxyapatite and Whitlockite can provide enhanced biological

responses such as cell adhesion, proliferation, and differentiation, which are important for promoting tissue growth and healing[28].

In addition, the use of nanocomposites in scaffolds can also provide specific functionalities such as drug delivery and imaging capabilities as shown in Figure 10. For example, nanoparticles can be incorporated into the scaffold to release growth factors or drugs in a controlled manner to improve tissue regeneration.

Overall, nanocomposite scaffolds help in tissue engineering and regenerative medicine because of their ability to enhance the properties of scaffolds and give additional functionalities[29].

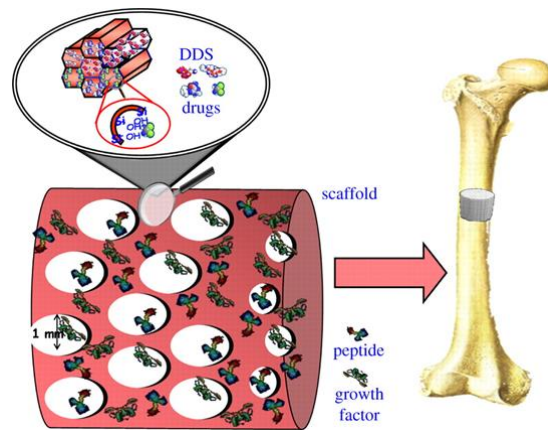


Figure 2.9: Scaffolds for bone tissue regeneration

2.4.3 Coating of implants

The mineral hydroxyapatite (HA) is frequently utilized as a bone substitute material or implant covering due to its outstanding osteoconductivity and resorbability. Both metallic and ionic silver are thought to have a wide range of antibacterial characteristics, especially when it comes to illnesses connected to biomaterials[30]. By immediately releasing antimicrobial agents to limited areas, such as the implant tissue interface, hydroxyapatite containing antimicrobial agents is predicted to prevent or treat implant-associated infections. Studies have shown that covering implant surfaces with antibiotics is a simple process[30].

2.5 What are Nano composites?

The term Nano composites has gained significant importance in the recent years. It is due to their ability to encompass various systems like 1-D, 2-D, 3-D and amorphous materials which are being formed with different components but in nanometer scale. Clay, carbon, polymers, or mixtures of these materials with nanoparticle building blocks make up nanocomposites.

The ability to achieve control of the nanoscale structures via novel synthetic techniques is the subject of intense research. Nanocomposite materials qualities are influenced by their morphology and interfacial characteristics in addition to the characteristics of each of its individual parents.[31]

The creation of polymer nanocomposites is at the core of polymer nanotechnology. The addition of nanometric inorganic compounds enhances the properties of polymers and has a big range of uses, contingent upon the amount of inorganic material contained inside the polymers. Solvent casting is one of the easiest and fastest methods for producing polymer nanocomposites.[32]

2.5.1 *History of Biomedical nanocomposites*

Bionanocomposites, a class of hybrid materials made of organic and inorganic fillers and synthetic and natural biodegradable polymers. Applications ranging from bone tissue engineering to load-bearing composites for bone regeneration can be made using various chemistries and compositions. The interaction between the selected matrix and the filler is a crucial component behind the properties of biomedical nanocomposite materials.[33]

In the recent times some methods of synthesizing and developing properties of polymer nanocomposites and some bioactive ceramics have been used in bone tissue engineering. One of the examples is the use of scaffolds which are declared compatible by many researches.

MA Maghsoudlou et al. using a freeze-drying technique prepared, the bio-nanocomposite scaffolds of chitosan (CS), hydroxyapatite (HA), and wollastonite (WS), with incorporations of 0, 10, 20, and 30% of zirconium, were created in this study. Additionally, scanning electron microscopy, energy dispersive spectroscopy, and x-ray diffraction (XRD) were used to examine the phase structure and morphology of scaffolds. The scaffolds' porosity in the body's typical bone region was discovered by examining the SEM pictures. The scaffolds' bioactivity and biodegradability were tested in the following stage. The bio-nanocomposite scaffolds were capable of adequately absorbing water since they contained hydrophilic components and had a high capacity for water absorption. The mechanical characteristics of the scaffolds were then investigated. [34]

Due to their alleged improved osteoconductivity, nanoscale bioactive glasses have recently attracted attention. Inorganic bionanomaterials are presented by Aldo et al., who used a variety of polymer matrices to create them, including polyesters like poly (hydroxybutyrate), poly (lactic acid), and poly (caprolactone), as well as natural-based polymers like starch, chitin, and chitosan, or proteins like collagen or silk fibroin. The benefits of incorporating nanoscale bioactive glasses in such biodegradable nanocomposites in terms of physico-chemical, mechanical, and biological aspects were discussed. [35]

2.5.2 Synthesis of biomedical application of nanocomposites with up conversion nanoparticles

The innovative idea of nanocomposite, which brings together several kinds of nanoparticles, has created new possibilities for managing more demanding properties for biomedical applications.

Besides their drug delivery potential, Noreen et al. explored and discussed different approaches for manufacturing multifunctional mesoporous silica nanocomposites. Multi-therapeutic delivery by mesoporous silica conjugated NPs can reduce toxicity while also improving delivery to the desired spot.[36]

Zhang et al. evaluated recent developments in nanocomposites made of MOFs and UCNPs for use in treatment, drug delivery, bioimaging, and biosensor applications. These findings demonstrate the usefulness of nanocomposites in biological applications by combining the porosity and structure-tunability of MOFs with the distinctive optical characteristics of UCNPs. Scientists are currently investigating additional synthesis techniques for biological applications in order to realise the potential application of MOFs-UCNPs nanocomposites.[37]

The aim of Jayalekhshmi et al.'s work was to create iron oxide-incorporated chitosan-gelatin bioglass composite nanoparticles (Fe-BG) that are both biocompatible and biodegradable created a composite nanoparticle and examined it using differential scanning calorimetry analysis (DSC), thermogravimetric analysis (TG), Fourier transform infrared (FTIR) spectroscopy, transmission electron microscopy (TEM), and X-ray diffraction (XRD). [38]

2.6 Application of Bioactive nanocomposites in Bone tissue regeneration

Here we enlist some literature regarding various applications of nanocomposite beads in tissue engineering field.

2.6.1 Bioactive nanocomposite scaffolds

Mozafari et al. cross-linked gelatin and nano bioactive glass to create mechanically effective and bioactive nanocomposite scaffolds using layer solvent casting, freeze-drying, and lamination processes. He created a novel composition to create a new bioactive nanocomposite with pores that range in size from 200 to 500 micrometres and a porosity of 72% to 86%. Additionally, the scaffolds' in vitro cytocompatibility was evaluated using the MTT assay and cell attachment research. Results showed no evidence of toxicity, and cells were discovered to be adhered to the scaffolds' provided pore walls. According to these findings, the created nanocomposite scaffold meets the requirements for bone tissue engineering scaffolds and can be applied to tissue engineering.[39]

Jayakumar et al. studied that due to the biocompatibility, biodegradability, and non-toxicity, as well as their antibacterial activity and low immunogenicity, chitin and chitosan

are suitable materials for biomedical applications. This obviously indicates an enormous potential for future development. These biopolymers may be processed quickly to create scaffolds in the shape of gels, sponges, membranes, beads, and more. The preparation and uses of chitin and chitosan based nanofibers, nanoparticles, and nanocomposite scaffolds for tissue engineering, wound dressing, drug delivery, and cancer diagnosis were highlighted by Jayakumar et al. in their emphasis on recent research on various aspects of chitin and chitosan based nanomaterials.[40]

2.6.2 Nanocomposite hydrogels for biomedical applications

Due to the porous and wet molecular structure, hydrogels resemble the morphology of real tissue. With a focus on biomedical and pharmaceutical applications, Gaharwar et al. examined the most recent advancements in the field of nanocomposite hydrogels. He highlighted the creation of nanocomposite hydrogels in particular, looked at their current drawbacks, and offered future options for developing more sophisticated nanocomposite hydrogels for medicinal and biotechnological applications.[41]

The most recent developments of nanomaterials composite hydrogels in biomedicine, such as drug and cell delivery, cancer treatment, tissue regeneration, biosensing, and bioimaging, were thoroughly summarised and discussed by Huang et al. They also briefly touched on the current state of their commoditization in the field of biomedicine. He spoke about the most recent developments in nanomaterials composite hydrogels used in biomedicine, such as new technology for nanocomposite hydrogels, nanocomposite hydrogels that can be injected and have advantages over traditional hydrogels in terms of minimally invasive surgery, self-healing, and bioimaging. The applications examined here cover nearly all facets of biomedicine, including tissue regeneration, cancer treatment, drug and cell delivery, biosensing, and bioimaging.[42]

Injectable hydrogel scaffolds that use minimally invasive implantation techniques to effectively mend and regenerate damaged bone structures. These scaffolds have a number of benefits since they can be injected into the irregularly shaped defect and operate as a low-density aqueous reservoir, containing the essential elements for bone tissue regeneration and augmentation. Injectable hydrogels' polymer matrix, property

specifications, and crosslinking methods were discussed by Phogat et al. gave several methods for creating injectable composites with a focus on nanocomposite hydrogels that incorporated bioinert and bioactive nanofillers. The underlying difficulties in creating injectable hydrogel nanocomposite scaffolds as well as the scientific efforts made to address these issues have been discussed.[43]

2.6.3 Polymeric nanocomposite beads for Drug Delivery application

The composition and production of hydrogel beads were investigated by Amiri et al. Due to their well-known biocompatibility; hydrogels are frequently used as a host (or drug carrier) in drug delivery. Due to their unique physical, chemical, and biological characteristics, hydrogels are used widely in many fields. Hydrogels are commercialized/produced as both natural and manufactured crosslinked hydrophilic polymers. These polymers can potentially be employed for biomedical treatments because they are compatible with human tissues. [44]

According to numerous documented studies, chitosan has been employed for a number of medicinal applications during the past few decades, including antibacterial, antioxidant, anti-inflammatory, anticancer, and drug delivery systems. There is also much discussion of a variety of chitosan sources, modification processes, and manufacturing techniques. According to Kedir et al., who cited a wealth of recent publications, chitosan and its nanocomposite have a promising future thanks to improved distinctive qualities such as their especial biocompatibility, biodegradability, mechanical and thermal stabilities, barrier, and nontoxicity. This suggests their uniqueness in the biomedical application.[45]

2.6.4 Alginate composite systems as sustained drug delivery carriers

Sukhudub et al and his fellow researchers looked at how silver ions affected the shape and antibacterial abilities of hydroxyapatite-silver (HA-Ag) and hydroxyapatite-alginate-silver (HA-Alg-Ag) nanocomposites. SEM, TEM, X-ray diffraction, and Fourier transform infrared spectroscopy were used to examine the microstructure and phase

composition of the produced nanocomposites, and the development of the crystalline phase of Ag_3PO_4 was demonstrated.[46]

Alginates (salts of alginic acids), according to research by Das et al., are a class of naturally occurring biodegradable and biocompatible polymers. In the biomedical and pharmaceutical industries, alginates have long been the most frequently utilised excipients for biopolymeric groups. For the prolonged release of drugs, a variety of alginate-based composite particles have already been studied during the past few years. Alginate-MMT composites for sustained release drug administration are made by conjugating inorganic minerals like montmorillonite (MMT) with alginate matrices. He researched the applicability of alginate-MMT composites for sustained drug delivery systems and the conjugation of MMT with alginate matrices to create them.[47]

2.7 Hydroxyapatite-Alginate based Nanocomposite beads for drug delivery application

Sangeetha et al. investigated the effect of alginate on hydroxyapatite (HA) reinforced gelatin composites, which they identified as attractive candidates for synthetic bone grafts. Furthermore, ciprofloxacin and rifampicin-loaded bone grafts with sustained and prolonged release behaviour have been produced, and the amount of drug release from the matrix can be easily changed by modifying the graft composition during synthesis. It was discovered that as alginate was added to the matrix, the release rate increased and lasted for up to ten days. The higher fracture toughness provided by the inclusion of alginate allows the samples to be employed in orthopaedic applications. All of the samples demonstrated high bioactivity, cytocompatibility, and antibacterial activity against the bacteria which cause bone infections. [48]

Nayak et al. and Amit et al. studied that Hydroxyapatite (HAp) is a naturally occurring biocompatible bioceramic material that is extensively used in a variety of biomedical applications, including in tissue engineering, orthopaedics, dentistry, and drug delivery. Different biopolymers are being added to HAp to increase its use. Different alginate-based systems have been supplemented with HAp particles (both synthetic and naturally produced) to load a range of medication candidates. The majority of the reported

drug-releasing HAp-alginate based matrices were made using an ionic-gelation of sodium alginate procedure, which was then followed by air drying or spray drying. Since HAp-alginate systems minimise the shortcomings of pure alginate matrices (such as burst drug-releasing and low mechanical property in the alkaline pH), they have already been demonstrated to be effective for loading a range of medicines and resulting in sustained drug delivery.[49]

In order to address the issue of burst release in drug release from hydrogel matrices that are commonly used, Zhang et al. developed a novel method of preparing pH-sensitive sodium alginate/hydroxyapatite (SA/HA) nanocomposite beads. This was achieved by creating HA micro-particles in situ during the sol-gel transition process of SA. The objective of this work is to find a novel approach for reducing drug release and resolving the issue of medicines releasing suddenly from frequently used hydrogel matrices. The pH-sensitive SA/HA nanocomposite beads could be used to create medicinal formulations for oral administration.[50]

Fan et al. studied the in situ production of HA nanoparticles during the sol-gel transition of the SA/HNTs mixture which resulted in diclofenac sodium-loaded sodium alginate/hydroxyapatite/halloysite nanotubes (SA/HA/HNTs-DS) nanocomposite hydrogel beads. FT-IR spectroscopy, thermogravimetric analysis, and field emission scanning electron microscopy, among other techniques, were used to characterize the nanocomposite beads. The tubular structure of the HNTs and the in situ-formed HA nanoparticles limited the movability of the SA polymer chains, that is why the drug loading and release behaviour was improved.[51]

Sukhodub et al. created antibacterial HA/Alg/CHX scaffolds for biomedicine, namely for oral hygiene and prospective dental treatment in the form of a paste. He created a hydroxyapatite (HA), sodium alginate (Alg), and CHX composite biomaterial that can be employed as a carrier system for local medication administration, particularly in dental applications. The ability of a HA/Alg/CHX composite to function as slow release drug delivery systems in phosphate-buffered saline (PBS) was assessed using high-performance liquid chromatography.[52]

Onoyima et al. studies on Doxorubicin (DOX) (an anticancer medication) and its release kinetics and mechanism from hydroxyapatite-sodium alginate nanocomposites (HASA). Wet chemical precipitation was used to prepare hydroxyapatite (HA) in the presence of sodium alginate (SA). The drug loading was done at neutral pH, and the in vitro drug release was done in synthetic body fluid (SBF) at pH 7.4 and 37 °C. DDSolver software, an Excel add-in, was used to fit the release experimental data into model-dependent and model-independent techniques. The release half time (t_{50}) rose as the SA concentration increased. Except for HA and HASA-1%wt, first order kinetics best describes the release of DOX from other formulations.[53]

2.8 Whitlockite nanocomposites for biomedical applications

Hafezi et al. investigated merwinite and whitlockite powders synthesised using sol-gel and solid-state reactions, respectively. After soaking in SBF, sintered merwinite-whitlockite nanocomposites can generate bone-like apatite. The capacity of the composites to generate apatite was increased by increasing the merwinite content. Additionally, osteoblasts spread readily on the surface of merwinite-whitlockite nanocomposites. And came to the conclusion that they could be a good candidate for bone replacement. required to investigate these composites suitability as implant materials. [54]

Yegappan et al created an injectable carrageenan nanocomposite hydrogel with whitlockite nanoparticles and dimethyloxallylglycine, an angiogenic agent. SEM, TEM, EDS, and FTIR were used to characterise synthesised whitlockite nanoparticles and nanocomposite hydrogels. The hydrogels developed were injectable, physically stable, cytocompatible, and had improved protein adsorption. The incorporation of dimethyloxallylglycine resulted in an initial burst release followed by a 7-day continuous release.[55]

Nazir et al. in this paper described the synthesis and characterisation of nanohydroxyapatite (nHA) and nanowhitlockite (nWH), which were then inserted into poly-L-lactic acid (PLLA) to investigate their impact on its structure, mechanical characteristics, antibacterial potential, and cytotoxicity. SEM pictures of PLLA-nHA and PLLA-nWH demonstrated homogeneous nanoparticle dispersion in polymer. FTIR

spectroscopy revealed a shift in functional group position and suggested that PLLA' was transformed into more crystalline PLLA, which was confirmed by X-ray diffraction. It was clearly noted that the binary system PLLA-nWH showed good dispersion and interfacial interaction at all concentrations, leading in improved mechanical and enhanced osteoconductive capabilities when compared to PLLA-nHA.[56]

Whitlockite bioceramic nanoparticles (WH NPs) were produced by Amirthalingham et al. and included because they give better osteogenic stimulation compared to hydroxyapatite by giving increased local ion concentration. Simvastatin, a medication that stimulates the expression of BMP-2 and hence provides an environment for bone regeneration, was also added into the hydrogel system. Both WH nanoparticles and simvastatin might improve bone regeneration capability. The whitlockite nanoparticles were synthesised and characterised using a precipitation technique. SEM, FTIR, and rheological analysis were used to characterise the nanocomposite hydrogel system. The oxidised alginate-gelatin/WH NPs hydrogel system containing simvastatin has the potential to be exploited as a mending and regenerative system in cranial bone deformities.[57]

2.9 Objectives

After successful and thorough literature review we concluded that a comparison between different drug i.e. Ciprofloxacin loading in hydroxyapatite and whitlockite nanocomposite beads for effective drug delivery and release in vitro has not been studied earlier. The following objectives were achieved to design a therapeutic, bioceramic drug loaded nano composites and a comparison has been made herewith.

- Synthesis and characterization of Hydroxyapatite and Whitlockite nanoparticles.
- Different concentration of drug loading
- Preparation of Ciprofloxacin loaded Hydroxyapatite/Whitlockite-Alginate composite Beads
- Chemical characterizations of nanocomposite beads

- FT-IR Analysis
- Scanning electron microscopy
- XRD Analysis
- Raman Analysis
- Physical Testing (swelling behaviour)
- Drug release in-vitro studies

Recording and interpretation of the data collected via characterization techniques and comparative analysis of Hydroxyapatite-alginate and Whitlockite-alginate nanocomposites in biomedical applications was done which is explained well in the coming chapters.

CHAPTER 3: MATERIALS AND METHODS

Following materials and chemicals were required to carry out the synthesis process:

- Magnesium Hydroxide (Duksan, Korea)
- Calcium Hydroxide (GPR Rectapur, Belgium)
- Orthophosphoric acid (Honeywell, Germany)
- Ethanol (Sigma-aldrich Germany)
- Hydroxyapatite (HA) (Functional Materials lab)
- Calcium Chloride (Duksan, Korea)
- Sodium Alginate (Daejun, Korea)
- Deionized water (DI)
- Distilled water
- Phosphate Buffer Saline (Invitogen, USA)
- Ciprofloxacin (CPX)

The synthesis details about each step are explained below:

3.1 Synthesis and characterization of Hydroxyapatite nanoparticles

The wet chemical precipitation process was used to create hydroxyapatite (HA). Ca(OH)_2 and H_3PO_4 solution were prepared according to 1.67 Ca/P ratio. The required amount of Ca(OH)_2 mixture was taken and added in water heated at 100 °C in oil bath. The whole mixture was stirred for 20 minutes to ensure complete dispersion of Calcium Hydroxide in water. After that H_3PO_4 was added to the Ca(OH)_2 solution at a rate of 5 ml/5 min till pH 10. The entire mixture was then left to stir at 100 °C for four hours. The

mixture was taken out of the oil bath after four hours and left to cool at room temperature. To separate the product, the mixture was centrifuged for 10 minutes at 4500 rpm once it reached room temperature. After three rounds of washing in de-ionized water, the product was left to dry overnight at 70 °C. The dehydrated item was annealed at 950 °C for 4 h to obtain crystalline HA nanoparticles.

To determine the composition of the crystalline phase, XRD technique was used. The product's shape and crystal structure were examined using the JOEL JSM-6490LA SEM instrument.

FTIR analysis was done to examine the functional groups found in the hydroxyapatite. The room temperature was used for the micro-Raman scattering tests.

3.1.1 Drug loading

Ciprofloxacin hydrochloride was dissolved in distilled water before being loaded onto hydroxyapatite nanoparticles. Ciprofloxacin concentration is varied accordingly. We loaded the drug to maximum concentration i.e. 0.1g as reported in literature this is the maximum amount of drug that can be loaded in ceramic matrix. Further increase in drug concentration leads to agglomeration of solution. Hydroxyapatite powder was added to the drug solution in constant ratios and swired for 40 minutes at 60° C using a magnetic stirrer. The solution was then left undisturbed overnight. The suspension was then centrifuged next day for 5 minutes at 2000 rpm to separate the supernatant and precipitates were separated. The quantity of drug loaded on HA NPs surface was determined by finding the difference in drug concentration in the aqueous solution before and after loading.

Percentage of drug loading is calculated using the equation:

$$\text{Percentage of Drug Loading} = \frac{A-B}{A} * 100$$

Where A and B represent the initial and final drug concentration of the aqueous drug solution.

3.1.2 Preparation of Ciprofloxacin loaded Hydroxyapatite-Alginate composite

Ciprofloxacin-loaded HA powder was gently stirred into a Na-alginate solution until a homogenous paste was produced. The Ciprofloxacin-loaded Hydroxyapatite powder was combined with 1 to 3.0% w/v sodium alginate solution in a weight ratio of 40 wt% hydroxyapatite/alginate. The pastes were dropped into a 2 M CaCl₂ cross linking solution, where spherical-shaped particles formed instantly and were allowed to settle and become hard for 30 minutes. Following the gelling phase, the microspheres were collected and washed in water to eliminate any excess CaCl₂. Sample was dried overnight in a vacuum oven set to 30°C.

Table 3.1: Drug loading in percentage for Hydroxyapatite-Alginate composite with different drug concentrations.

Sr. No.	Hydroxyapatite loaded drug powder to alginate ratio	Drug ratio	g of HA/g of Alginate
1.	1:1	0.1%	40 wt %
2.	1:1	0.07%	40 wt %
3.	1:1	0.05%	40 wt %
4.	1:1	0.03%	40 wt %

3.1.3 Drug Release

To study the release profile of the drug, 100 mg of drug-loaded hydroxyapatite and drug-loaded hydroxyapatite with alginate coating were placed in a screw-capped glass container containing 50 ml of phosphate buffered saline (PBS) medium under sterile conditions at 37 °C and pH 7.4.

The medication release investigation was carried out over a 24-hour period. To obtain an accurate drug release study, the sample vials were shaken for 15 minutes prior to each reading. A pipette was used to remove 5 ml samples and immediately replace them with 5 ml of new PBS medium. The concentration of ciprofloxacin in the obtained samples was determined spectrophotometrically at a wavelength of 274 nm.

3.2 Preparation of Whitlockite based Nanocomposite beads

For synthesis of Whitlockite nanoparticles liquid precipitation method was carried out and for the synthesis of polymer nanocomposite crosslinking method was employed. Details are shared below:-

3.2.1 Synthesis and characterization of Whitlockite nanoparticles

The synthesis of Whitlockite nanoparticles was done at lab scale using already reported precipitation method reported by Batool et al. at Functional Materials Lab. In this method we used 0.13M Magnesium Hydroxide ($\text{Mg}(\text{OH})_2$) solution and 0.37M Calcium Hydroxide ($\text{Ca}(\text{OH})_2$). Stirring was done for 20 min at 40 ° C and then 0.5M orthophosphoric acid was added dropwise with feed rate 10ml/5minute until pH 5 of solution was obtained.

Further, condensation reaction takes place for 10 hours followed by aging of sample for about 14 hours. The obtained product was separated by filtration method. The precipitates were washed thrice to remove any unreacted components. The obtained sample was dried in vacuum oven at 50°. Dried sample was then converted into fine powder by grinding in mortar pestle and stored in vials for further characterizations.

Powder X-ray Diffract meter (XRD) present at SCME was used to study the crystalline phase composition. The morphology and crystal structure of the product were observed by JOEL JSM-6490LA SEM at SCME.

The functional groups present in samples were analyzed by FTIR. The micro-Raman scattering experiments were carried out to determine vibrational modes.

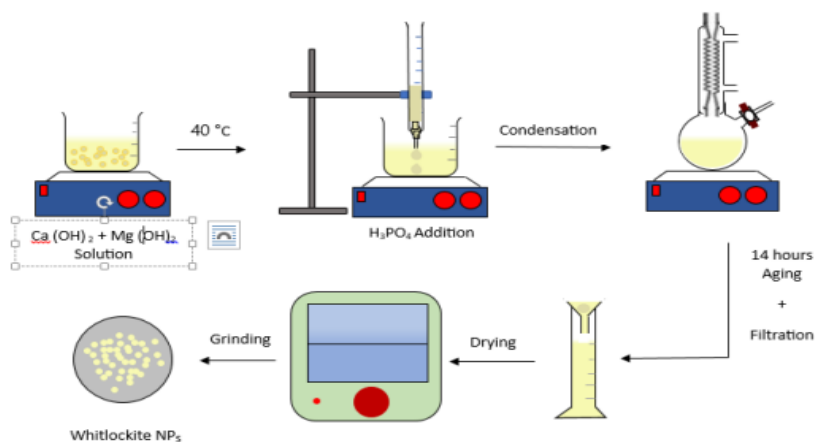


Figure 3.1: Schematics of Whitlockite synthesis

3.2.2 Drug loading

Ciprofloxacin hydrochloride was dissolved in distilled water and used to load medication on Whitlockite nanoparticles. Ciprofloxacin concentration is varied. A magnetic stirrer was used to stir whitlockite nanoparticles into the drug for 40 minutes at 60 °C. The solution was then left undisturbed for the following day. The supernatant and precipitate were then removed from the suspension using a centrifuge (2000 rpm, 5 min). By comparing the drug concentration in the aqueous solution before and after loading, the amount of drug loaded was calculated. Percentage of drug loading is calculated using the equation 3.2:

$$\text{Percentage of Drug Loading} = \frac{A-B}{A} * 100 \quad (3.2)$$

Where A and B represent the initial and final drug concentration of the aqueous drug solution.

3.2.3 Preparation of Ciprofloxacin loaded Whitlockite-Alginate composite

Whitlockite powder that had been loaded with ciprofloxacin was dissolved in a Na-alginate solution while being gently stirred until a homogenous paste was produced. The

weight ratio of Whitlockite to alginate was 40 weight percent, and the Ciprofloxacin-loaded Hydroxyapatite powder was combined with 1 to 3.0% w/v of sodium alginate solution. In a 2 M CaCl₂ cross-linking solution, the pastes were extruded drop by drop.

Instantaneously, spherical particles formed and were left to solidify for 30 minutes. The microspheres were collected once the gelling phase was over and rinsed in water to get rid of any extra CaCl₂. They were then dried for the entire night at 30 °C in a vacuum oven.

Table 3.2: Drug loading in percentage for Whitlockite- Alginate composite with different drug concentrations.

Sr. No.	Whitlockite loaded drug powder to alginate ratio	Drug ratio	g of WH/g of Alginate
1.	1:1	0.1%	40 wt %
2.	1:1	0.07%	40 wt %
3.	1:1	0.05%	40 wt %
4.	1:1	0.03%	40 wt %

3.2.4 Drug Release

In order to study the drug release profile, 50 ml of phosphate buffered saline (PBS) medium at 37 °C and pH 7.4 under sterile conditions was placed into a screw-capped glass container containing 100 mg of drug-loaded Whitlockite and drug-loaded Whitlockite with alginate coating in order to study the drug release profile. 24-hour interval was used for the medication release study.

To obtain an accurate drug release study, sample vials were shaken for 15 minutes prior to each reading. A pipette was used to remove 5 ml of the samples, which were then promptly replaced with 5 ml of brand-new PBS medium. This volume was taken into consideration when determining the amount released. At a wavelength of 274 nm, the concentration of ciprofloxacin in the samples was determined spectrophotometrically.

CHAPTER 4: CHARACTERIZATION TECHNIQUES

SEM was used to study the morphology of the samples using a JEOL JSM-6490A (Tokyo, Japan) with a combined EDAX EDS probe for elemental analysis. X-ray diffraction (XRD) was used to analyse the structural information on a Seimens D5005 STOE & Cie GmbH (Darmstadt, Germany) at an angle (2θ) ranging from 20° to 100° . FTIR analysis was performed using potassium bromide pellets and dried powder samples on a PerkinElmer SpectrumTM100 spectrophotometer. Raman spectra were acquired using a BW TEK INC (Newark, NJ, USA) BWS415-532S-iRaman. OPTIMA (SP-3000DB) UV-Vis spectrophotometer was used to study the Drug release efficiency of the samples. The drug release study was carried at 274nm.

4.1 Scanning Electron Microscopy

Using a concentrated electron beam to scan a sample, scanning electron microscopy, or SEM, creates images of the material. When electrons contact with atoms in a sample, they generate a variety of signals that are picked up and utilised to build an image. To increase the sample surface's electron conductivity and prevent over charging effect in SEM, a tiny layer of conductive material, like gold, is first applied to it. Next, a high-energy electron beam is used to scan the sample inside the microscope. Secondary electrons, backscattered electrons, and other signals are produced by the electrons' interactions with the sample's atoms. The signals are detected by a series of detectors, and the data is processed to create an image of the sample surface. SEM can produce high-resolution images with magnifications ranging from a few times to over a million times the original size of the sample. The technique is commonly used in materials science, biology, and

other fields to study the surface morphology and composition of samples. SEM can resolve materials that are both conductive and non-conductive. If an EDS detector is connected to the setup, elemental analysis of the material can be performed. It can provide quantitative as well as qualitative information about the material. To improve imaging, the samples are placed on a stub in the sample chamber and often sputtered with gold.

Here is a brief overview of how SEM machines work:

- **Electron gun:** SEMs use an electron gun to produce a beam of high-energy electrons that are accelerated towards the sample. The electron gun consists of a heated filament that emits electrons, which are then focused and accelerated by electromagnetic lenses.
- **Sample preparation:** The sample is initially prepared by coating it with a thin layer of conductive material, such as gold or carbon. This is necessary because the electrons in the beam are negatively charged and can't penetrate non-conductive materials.
- **Scanning:** A raster pattern or a sequence of lines is created as the electron beam scans across the sample's surface. The atoms in the sample interact with the beam as it scans the surface, causing them to release signals such as backscattered electrons and secondary electrons.
- **Imaging:** The electrical signals are then processed by a computer, which generates a high-resolution image of the sample surface. The image shows the

variations in the intensity of the signals, which correspond to the topography and composition of the sample.

SEM machines can provide extremely high-resolution images, with magnifications ranging from 10x to over 1,000,000x, and are used in scientific and industrial applications, such as materials science, biology, geology, and nanotechnology.

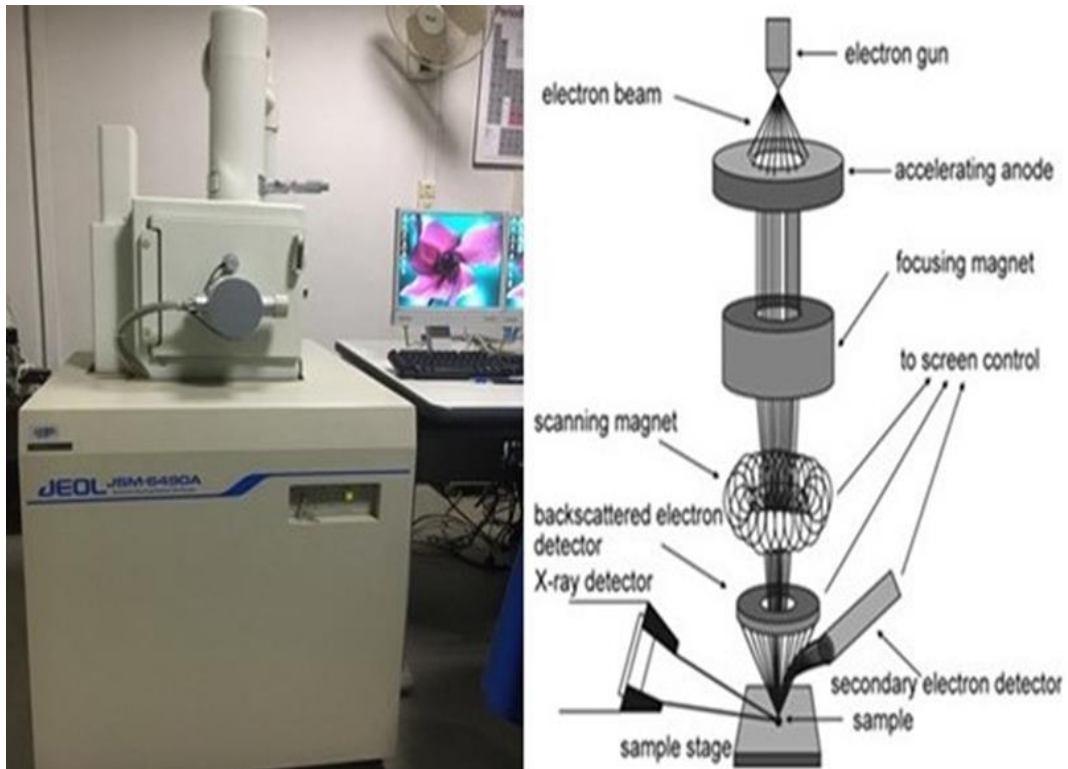


Figure 4.1: (a) JOEL JSM-6490LA SEM at SCME; (b) Schematics of SEM

4.2 X-ray diffraction (XRD)

It is used for the elucidation of the phase purity and crystallographic orientation of the material. It delivers fingerprints of Bragg's reflections of crystalline materials. X-rays are produced by heating filament element which accelerates electrons towards a target

which collide with target material with electrons. As a crystal is composed of layers and planes so, x-rays which have wavelength similar to these planes is reflected at that angle of incidence which is equal to the angle of reflection. “Diffraction” is observed, and it can be described as by Bragg’s Law shown in equation 4.1.

$$2 d \sin \theta = n\lambda \quad (4.1)$$

Constructive interference is seen when Bragg’s law satisfied, and “Bragg’s reflections” will be picked up by the detector. These reflections positions tell us about inter-layer spacing-ray diffraction tells us about the phase, crystallinity, and sample purity. By this technique, one can also determine lattice mismatch, dislocations, and unit cell dimensions. X-ray diffractions were accomplished by using STOE diffractometer at XRD Lab SCME-NUST. The scan angle was taken in 2θ and samples were scanned from 20° to 80° with a scan rate of 0.02° .

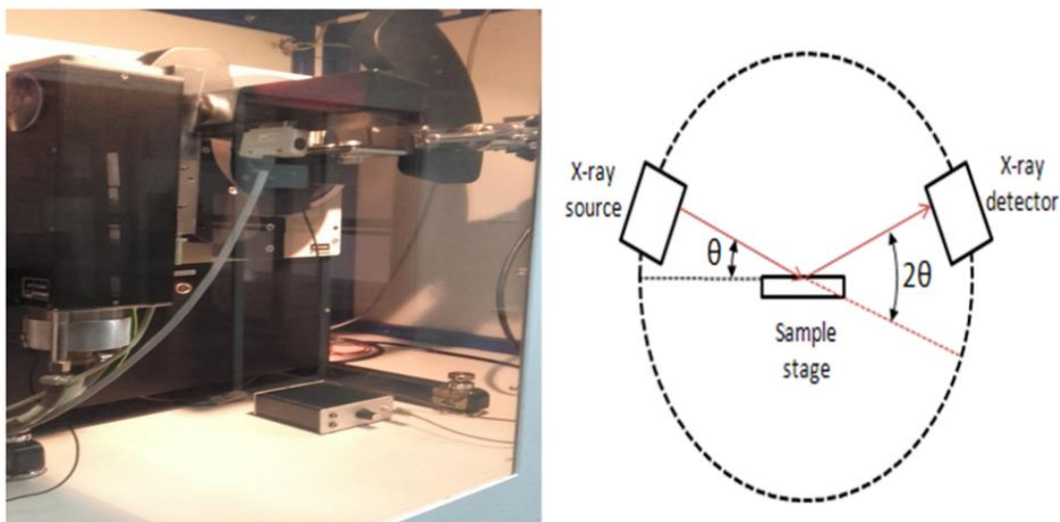


Figure 4.2: XRD present at SCME-NUST (b) XRD basic schematics

4.3 Fourier Transform Infrared (FT-IR) Spectroscopy

Infrared spectroscopy investigates the interaction of infrared radiation with materials. Infrared radiation is a type of electromagnetic radiation having a longer wavelength than visible light. When infrared rays are absorbed by molecules within a substance, the radiation energy absorbed is equal to the vibrational transition energy. As this vibrational energy is also connected with different rotational energies, the band shape following IR absorption is provided. These vibrational transitions are recorded as peaks and are observed in the 4000-1300 cm^{-1} range. Single bonded atoms extend approximately 4000-2500 cm^{-1} , and if there is hydrogen bonding in this region, a broadening of peaks will be noticed.

The molecular vibrations produced due to IR interactions will be of two types. The change in types of vibrations are governed by structural geometry, position and orientation. For a linear geometry, bond stretching vibration will be generated. Stretching will be of two types:

- Symmetric
- Asymmetric

For any difficult and complex structure, the mode of vibration will be manifested in different kinds of bending movements which are:

- Scissoring
- Rocking

- Wagging
- Twisting

The Infrared IR region of the electromagnetic radiation is generally divided in 3 regions:

- Near IR
- Mid IR
- Far IR

FT-IR Spectroscopy can identify samples in any form. It is an effective analytical method for determining the identity and characteristics of chemical substances by analysing how well they absorb or transmit infrared light. A sample is exposed to an infrared laser beam during FTIR spectroscopy, and the spectrum that results is measured.

FTIR spectroscopy is a non-destructive and non-invasive analytical technique, making it a valuable tool in materials science and forensic analysis. It is also commonly used in quality control and process monitoring in manufacturing industries, such as the pharmaceutical and chemical industries.

FTIR spectroscopy measures the amount of radiation absorbed at different frequencies by sending an infrared beam through a sample. The sample, which is often a thin film, liquid, or gas, is placed in a sample holder that allows the infrared beam to flow through it. A beam splitter is then used to divide the infrared beam into two beams, one directed at the sample and the other at a reference detector. The sample absorbs some of

the infrared radiation, lowering the strength of the beam that passes through it. The intensity of the beam that has not interacted with the sample is measured by the reference detector. After then, the two beams are recombined and guided. The resulting signal is a plot of the amount of infrared radiation absorbed by the sample at different frequencies. The peaks in the spectrum correspond to the specific vibrations of the atoms in the sample. The position and intensity of the peaks provide knowledge about the types of bonds present and their environment in the sample.

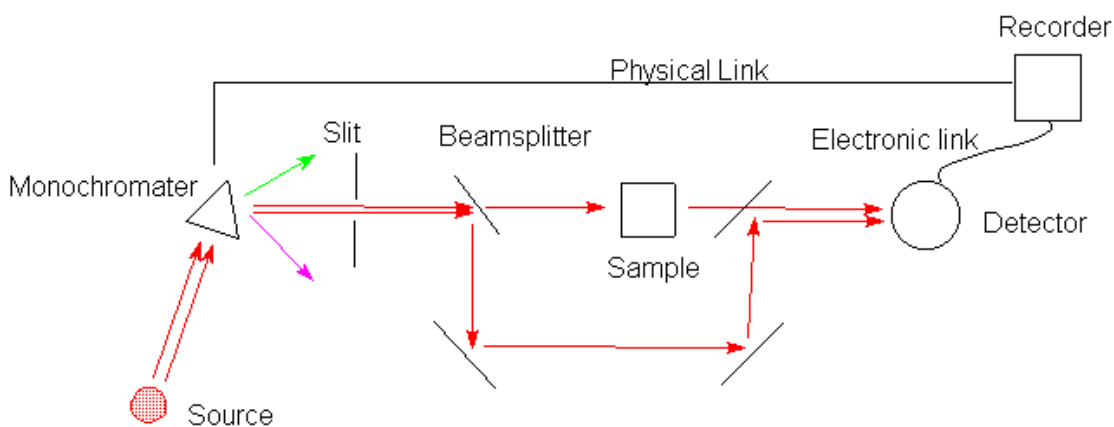


Figure 4.3: Working schematics of FT-IR Spectroscopy

4.4 Raman Analysis

Raman analysis is a spectroscopic technique used to study Raman scattering to determine the vibrational modes of molecules. The base of the inelastic scattering of monochromatic light, usually from a laser, of the sample. When the laser light interacts with the sample, some of the photons are scattered inelastically, meaning that the energy of the scattered photon is quite different from that of the incident photon. The difference in energy is related to the vibrational modes of the molecules in the sample.

In addition to its analytical applications, Raman spectroscopy is also used for imaging, where a Raman map of a sample is generated by scanning the laser across the sample surface and measuring the Raman spectra at each point. This can be used to create images that reveal the spatial distribution of different chemical components within the sample.

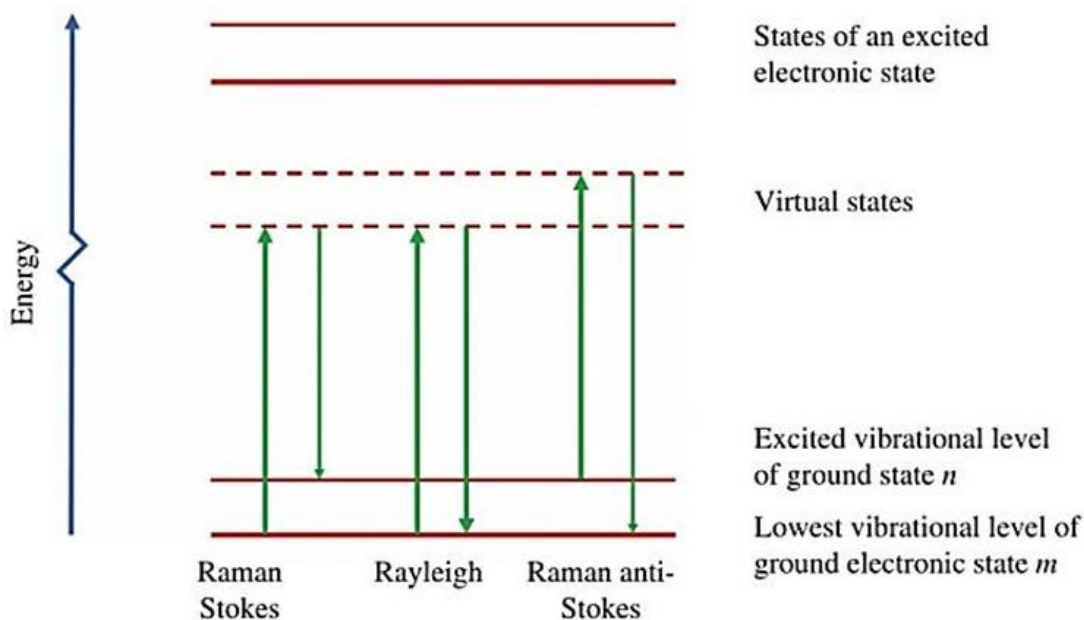


Figure 4.4: Schematics showing Raman scattering process

4.5 UV-vis Spectroscopy

UV-Vis spectroscopy is a technique that calculates how much light a material absorbs or transmits using ultraviolet and visible light. The Beer-Lambert rule, which states that the quantity of light absorbed by a sample is exactly proportional to the concentration of the absorbing species and the route length of the light through the sample, forms the foundation of UV-Vis spectroscopy's basic operating principle.

This technique includes measuring light absorption as a function of wavelength, which gives information about electron transitions in the material. It is a method for calculating the band gap when electrons move between the conductance and valence shells. It is based on the frequency relationship equation of Bohr and Einstein shown in equation 4.2:

$$\Delta E = E_2 - E_1 = h\nu \quad (4.2)$$

It connects molecular or discrete energy levels to electromagnetic radiation frequency. Here, h is Planck's constant, which is 6.626×10^{-34} Js, and in optical spectroscopy, wavenumber is preferred above frequency, hence the following equation 4.3 is used:

$$\Delta E = E_2 - E_1 = hc\bar{\nu} \quad (4.2)$$

The ultraviolet or visible portion of the electromagnetic spectrum is emitted by a light source and directed through a monochromator to pick a particular wavelength of light in a UV-Vis spectrometer. After the sample is exposed to the chosen wavelength of light, a detector measures how much of the light is absorbed or transmitted by the sample.

The detector converts the amount of absorbed or transmitted light into an electrical signal, which is recorded by a computer as a spectrum.

In order to detect the active pharmaceutical ingredient Ciprofloxacin (CPX) is present and released in suitable environment. UV-vis spectroscopy was performed at 276nm. Sample was prepared by adding the 10mg w/v nanocomposite beads in 10ml PBS

solution. Readings were taken in order to do a 24hour study. About 5ml of aliquots were taken from each vial and added to quartz crystal cuvette and placed in cell of UV-vis spectrophotometer Optima SP-3000 DB. The aliquot extracted is replaced with freshly prepared PBS solution to keep volume constant. After every reading the aliquot is discarded and is rinsed with DI water. During the entire experiment PBS solution is kept as reference in cuvette and placed in reference cell. Machine is auto-zeroed before taking each reading to get precise and accurate results.

This study is used in the fields of science, including chemistry, biochemistry, and environmental science, to identify and quantify various substances, such as chromophores, metal ions, and organic molecules. It is also used to study the kinetics of reactions and to determine the purity of a sample.



Figure 4.5: UV-vis spectrometer Optima SP-3000DB

4.6 Physical Characterization of Nanocomposite Beads

Physical Test (swelling test) was carried out to study the properties and evaluate the efficiency of Nanocomposite Beads.

4.6.1 Swelling Test

Nanocomposite beads have capability to absorb water and swell while maintaining their 3-D structure. In order to measure the extent of water absorption and swelling capacity of the nanocomposite beads, swelling test is performed in which sample beads 10mg weight and specific size are weighed. The samples are immersed in solvent that is PBS Solution for certain time and weight is measured again to determine change in weight and swelling capacity. Following formula is used to calculate swelling as shown in equation 4.3:

$$\text{Percentage swelling}(\%) = \frac{W_f - W_o}{W_o} * 100 \quad (4.3)$$

Where W_f is final weight and W_o is initial weight of sample beads. Percentage swelling was calculated using above mentioned formula.

CHAPTER 5: RESULTS AND DISCUSSION

Characterization Techniques for Hydroxyapatite and Whitlockite composites beads for sustained release of drug ciprofloxacin.

5.1 Fourier Transformation – IR (FTIR) Analysis

The synthesis of nanocomposite beads was carried out in 2 steps. First of all the addition of drug ciprofloxacin in bioceramic in adequate ratio as described earlier followed by addition of polymer sodium alginate. So we had to carry out characterizations for both the steps to confirm crosslinking between polymer and bioceramic and the drug.

5.1.1 FT-IR of Hydroxyapatite-Drug powder

In figure 5.1(a) the results of FT-IR analysis of drug loaded HA powder for different drug (CPX) concentration with fixed HA concentration have been reported here.

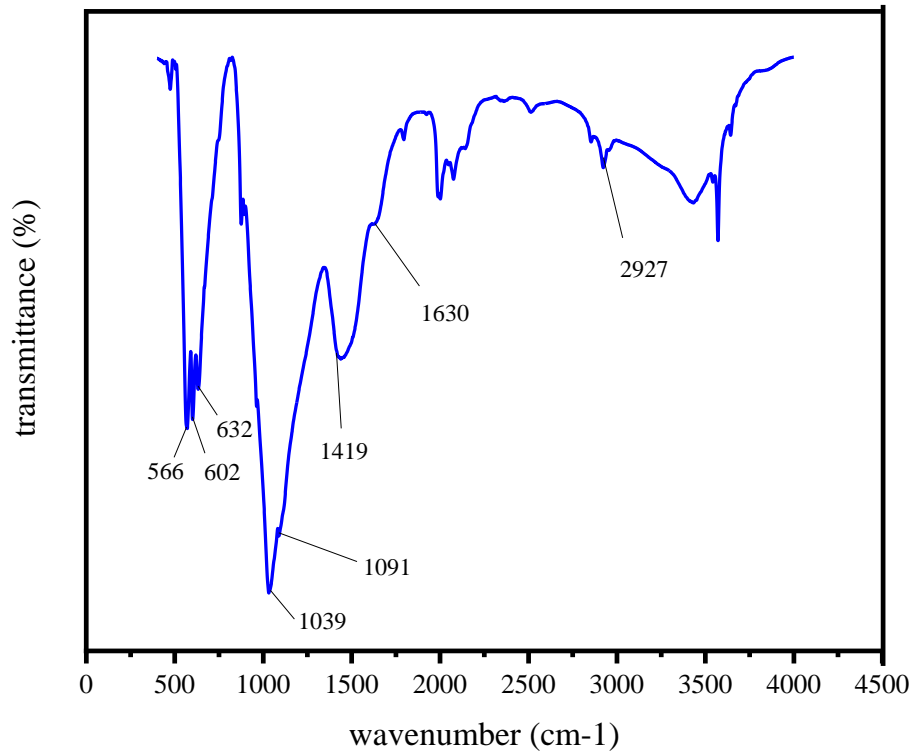


Figure 5.1: FTIR spectrum of pure HA

The existence of hydroxyapatite free of organic matter is indicated by the development of peaks 634.58 cm^{-1} , 601.79 cm^{-1} , and 570.93 cm^{-1} in the FT-IR spectra of pure HA, as shown in the figure below.

These peaks were caused by the symmetrical stretching of a phosphate group (PO_4^{3-}). The overtone combination bands, CH stretching (methylene), NCH₃ (methylamine), CC stretching (alkynes), and the regions with maxima at 2883.58 cm^{-1} , 2827.64 cm^{-1} , and 1990.54 cm^{-1} were identified, respectively. The CO_3 (carbonate group) has an asymmetric stretching and was identified as the cause of the bands at 1460.11 cm^{-1} and 1413.82 cm^{-1} .

Distinctive peaks of ciprofloxacin in the FT-IR spectra of the Hap ciprofloxacin powders either shifted very slightly or were exactly the same as the reference samples reported in the literature. This validates that ciprofloxacin is present in the HAp-system either with no interaction or very little interaction.

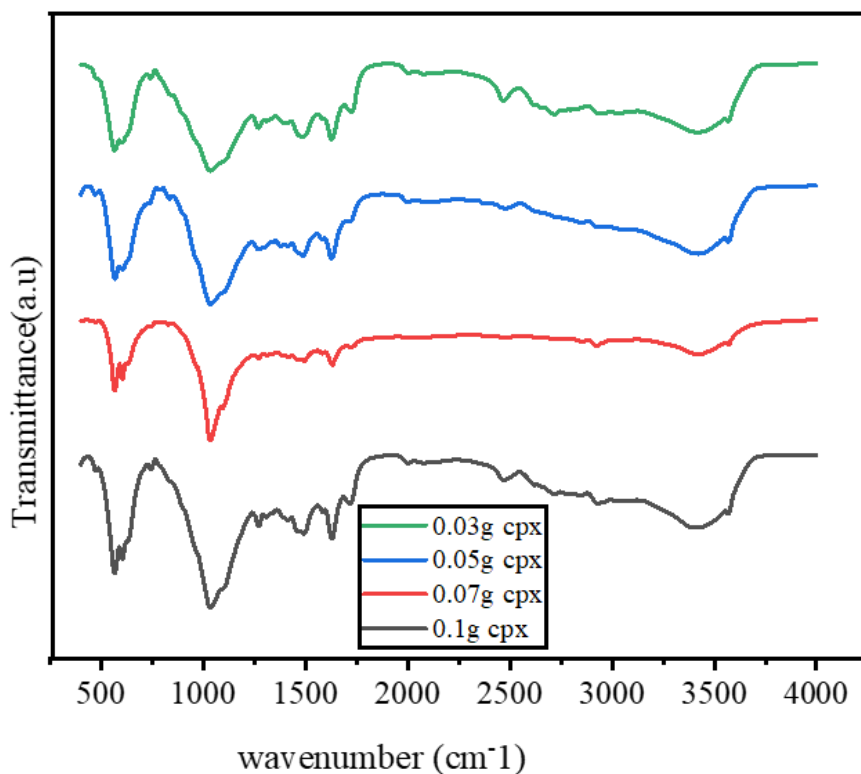


Figure 5.2: (a) FT-IR of Hydroxyapatite-Drug powder with different drug ratios.

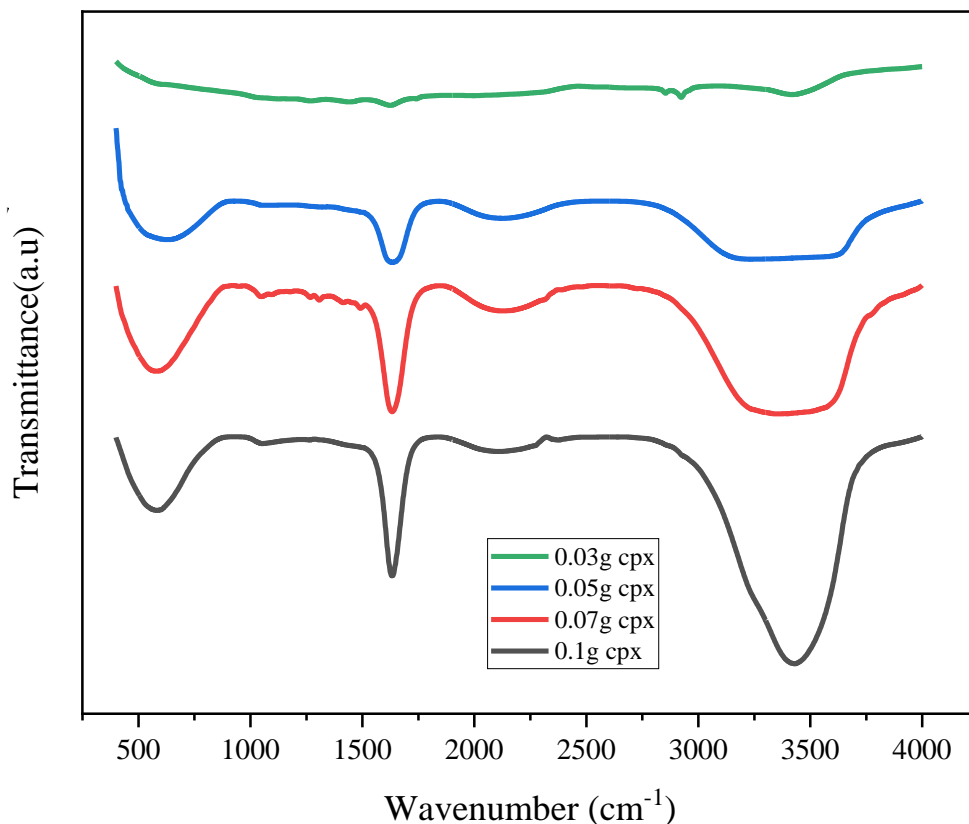


Figure 5.3: FT-IR of Hydroxyapatite-Alginate Nano composite beads loaded with different Drug ratios

FTIR spectroscopy was carried out to study structure of drug-loaded hydroxyapatite for same HA and varied CPX mass ratios.

The findings are displayed in figure 5.1. For every hydroxyapatite/drug sample, distinct structural bands of ciprofloxacin and hydroxyapatite were detected. The drug-loaded hydroxyapatite exhibits mixed bands characteristics of both ciprofloxacin (C-C bond stretching at 1608, C-H₂ bending at 1468, mixed vibrations at 1311, the C-H in plane bending at 1272, and C-N stretching was seen at 867) and hydroxyapatite (P-O at 566, 602, 962, 1091 and O-H at 632, 3564).

As the drug loading percentage rises, so do the associated band intensities increased.

5.1.2 FT-IR of Hydroxyapatite-Alginate Nano composite beads loaded with Drug

FT-IR spectrum of 4 samples having Ciprofloxacin loaded into hydroxyapatite-alginate nanocomposites is shown in Figure 5.2.

In case of Hydroxyapatite (HA) broad absorption bands were seen in the range of 3400-3200 cm^{-1} that indicates O-H stretching vibrations from surface hydroxyl groups and absorbed water. Bands around 1635 cm^{-1} , representing the bending vibration of water molecules. Phosphate (PO_4) vibrations:

A strong band at around 960 cm^{-1} corresponds to symmetric stretching (ν_1) vibrations of phosphate groups. Bands between 600-550 cm^{-1} (ν_4) and 1100-1000 cm^{-1} (ν_3) related to phosphate vibrations. Calcium-related bands: Absorption bands around 1450 cm^{-1} attributed to carbonate groups substitution in the HA lattice. Bands around 875 cm^{-1} confirmed bending vibration mode of carbonate ions.

Sodium Alginate: A broad band around the region of 3400 cm^{-1} indicating O-H stretching vibrations from hydroxyl groups and absorbed water. A strong peak at around 1600-1630 cm^{-1} representing the carboxylate group (COO^-) stretching vibration.

Bands between 1400-1500 cm^{-1} were associated with the asymmetric and symmetric stretching vibrations of COO^- groups. Bands at 1030 cm^{-1} corresponding to the C-O stretching vibrations in the saccharide ring of alginate.

When hydroxyapatite and sodium alginate are combined, you would expect to see a combination of the characteristic peaks from both materials in the FTIR spectrum.

Additionally, interactions such as hydrogen bonding or chemical bonding between the functional groups of the two compounds might result in shifts or changes in the intensity of certain peaks, providing information about their interaction in the composite material.

5.1.3 FT-IR of Whitlockite-Drug powder

FTIR spectra of whitlockite and ciprofloxacin powder was done and certain characteristic peaks were observed as shown in figure 5.3.

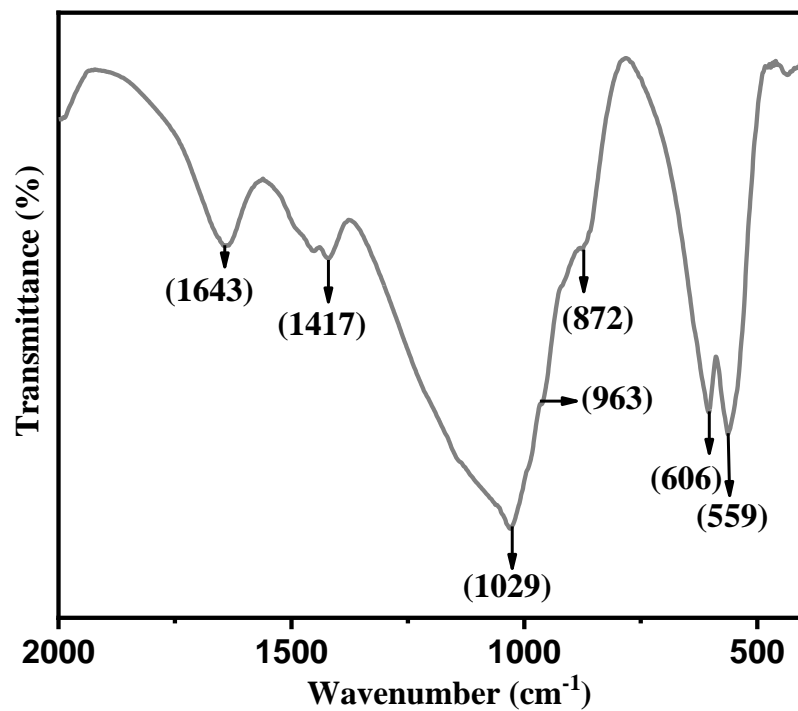


Figure 5.4: FTIR of PURE WH

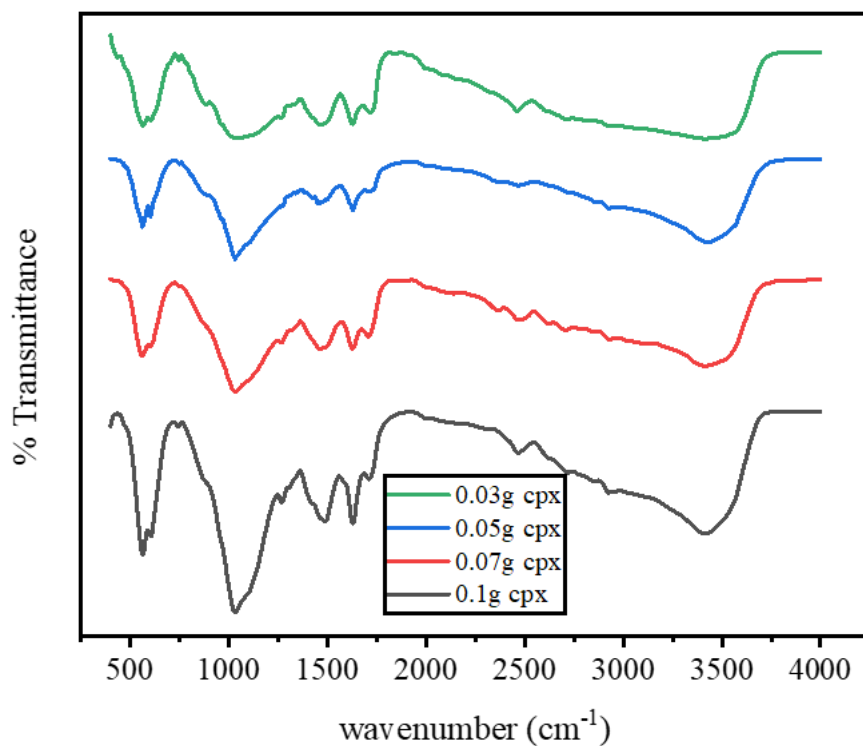


Figure 5.5: FT-IR of Whitlockite-Drug powder with different drug ratios

Figure shown above is the FT-IR spectrum of pure WH which is a calcium phosphate mineral, and its FTIR spectrum typically showed the absorption bands correlate with the phosphate groups (PO_4) and hydroxyl groups (OH^-). The specific peaks and their assignments might vary depending on factors like crystal structure and impurities, but generally, peaks were around:

Phosphate groups: These typically appeared in the region of $900\text{-}1200\text{ cm}^{-1}$, with specific peaks around 960 , 1020 , and 1090 cm^{-1} .

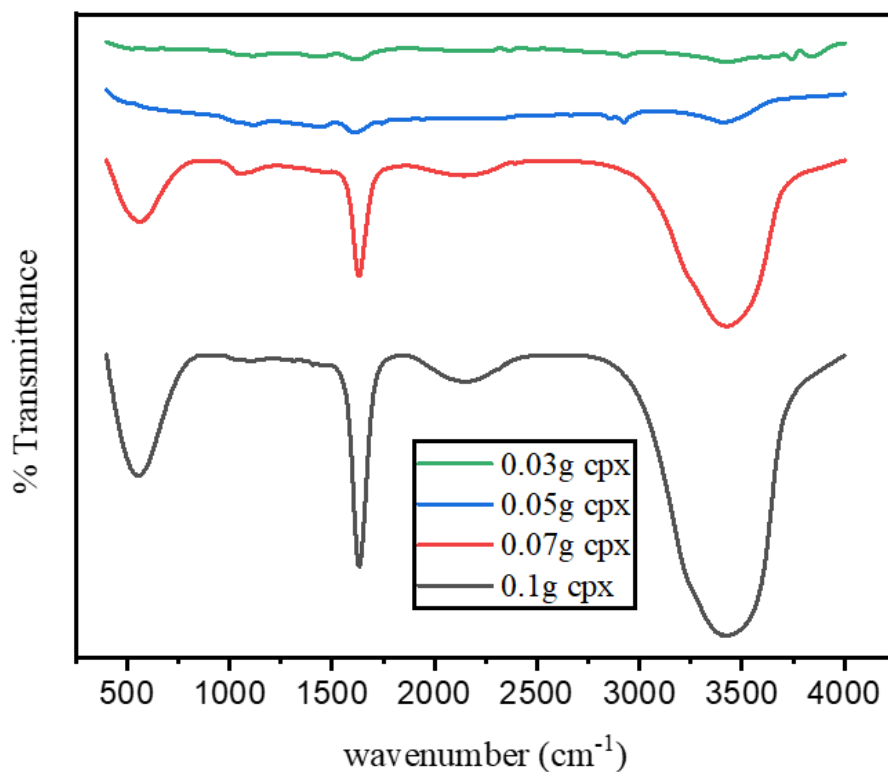


Figure 5.6: FT-IR of Whitlockite-Alginate nanocomposite beads loaded with different drug ratios

Hydroxyl groups: These usually appeared as a broad peak in the region of $3100\text{-}3600\text{ cm}^{-1}$

Ciprofloxacin is an antibiotic belonging to the fluoroquinolone class. Its FTIR spectrum will exhibit absorption bands corresponding to various functional groups present

in its molecular structure, such as: Amino groups (-NH₂): These typically appeared in the region of 3200-3500 cm⁻¹. Carbonyl groups (C=O): These appeared around 1650-1750 cm⁻¹. Fluorine-containing groups: Due to the presence of fluorine atoms in ciprofloxacin's structure, there were characteristic peaks in the region of 1000-1300 cm⁻¹. Piperazine ring: showed peaks around 1400-1600 cm⁻¹.

5.1.4 FT-IR of Whitlockite-Alginate Nano composite beads loaded with Drug

FTIR (Fourier Transform Infrared Spectroscopy) of whitlockite-alginate-ciprofloxacin beads of 4 samples was done to identify functional groups present in the compound. Here's a general overview of the peaks:

Whitlockite is a calcium phosphate mineral. In the FTIR spectrum, characteristic peaks related to phosphate groups (PO₄³⁻) and possibly calcium ions (Ca²⁺) were seen as shown in figure 5.4. The phosphate stretching vibrations typically occurred in the range of 1200-900 cm⁻¹.

Alginate peaks related to its functional groups were evident in the spectrum. Carboxylate groups (COO⁻) appeared around 1600-1400 cm⁻¹, and hydroxyl groups (OH) typically absorbed around 3400 cm⁻¹.

Ciprofloxacin is an antibiotic. Its FTIR spectrum showed peaks corresponding to various functional groups present in its chemical structure, such as amine (N-H) and carbonyl (C=O) groups. However, it was seen that all the required peaks were present in the spectra confirming the crosslinking between the polymer matrix and bioceramic. It was also seen that as the drug ratio was increased keeping the ceramic and polymer ratio constant sharp peaks emerged in the spectra. With the decrease in amount of drug loading the peak intensities also reduced.

5.2 X-ray Diffraction (XRD) Analysis

XRD Analysis of all the compositions for both the composites of Hydroxyapatite and Whitlockite was done to find out the crystal structure of the material. Our findings are summarized below:

5.2.1 XRD Analysis of Hydroxyapatite-Drug Powder

As in-depth study of the X-ray diffraction (XRD) spectra of four samples comprising of Hydroxyapatite and ciprofloxacin powder was done to study their structural peaks and to check whether the drug was successfully loaded onto the ceramic particles.

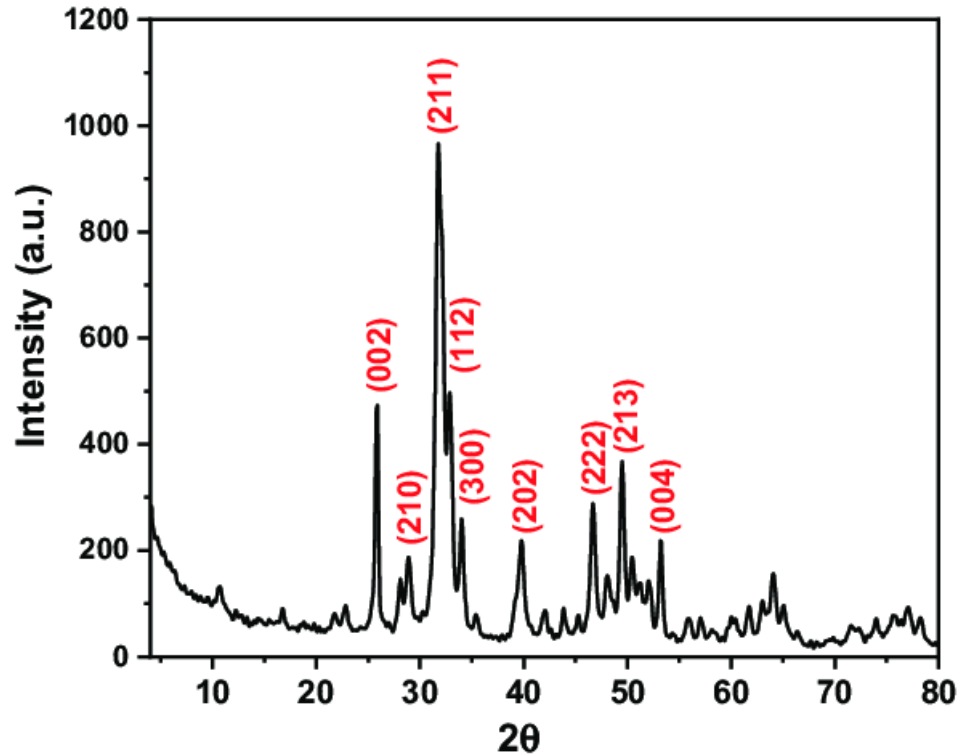


Figure 5.7: XRD of pure HA

X-ray diffraction (XRD) analysis of a mixture containing hydroxyapatite and ciprofloxacin would involve identifying the diffraction peaks corresponding to each substance. Hydroxyapatite, a calcium phosphate mineral, typically exhibits characteristic diffraction peaks around 2θ values of 25.9° , 31.8° , 32.2° , 32.9° , 39.8° , 46.8° , and 49.5° , corresponding to its crystal structure.

However, from reported literature it was studied that ciprofloxacin, being an organic compound, may not produce sharp diffraction peaks in XRD due to its non-crystalline or amorphous nature and the high intensity peak with hkl (2 1 1) was observed in n-Hap is shown in spectra. However, if the ciprofloxacin is in a crystalline form, it would

also exhibit characteristic diffraction peaks. According to the spectra we observed peaks of ciprofloxacin typically at $2\theta = 19.22^\circ$, 26.39° , and 29.16° which is also confirmed from the literature. So this data confirms that our drug is inserted into the bio ceramic, presence of these specific peaks in spectra show that Hydroxyapatite and drug are present in the powdered matrix. The samples having maximum drug content showed sharp peaks like the samples having 0.1g drug and 0.07g drug in figure 5.5. As the drug ratio is decreased the sharpness of peaks is also reduced. But the presence confirms that both are bonded successfully into each other.

5.2.2 XRD Analysis of Hydroxyapatite-Alginate nanocomposite beads loaded with Drug

The diffraction pattern that is produced while analyzing a mixture that contains both sodium alginate and HA is a composite of the peaks from both substances. The XRD pattern was normally dominated by the strong, well-defined peaks from HA, whereas the sodium alginate peaks were likely seen to be diffused or less noticeable in figure 5.6. It was easy to index and compare each of the observed peaks with the hexagonal HAp values that have been published (JCPDS file no. 09-0432). At $2\theta = 26.29$, 31.74 , 32.18 , 34.04 , 39.17 , 45.31 , 46.66 , 49.46 , 53.30 , 56.94 , and 64.12° , pure hydroxyapatite nanoparticles displayed diffraction peaks, signifying matching indices of (002), (211), (112), (202), (212), (203), (222), (213), (004), (114), and (323), respectively.

The peaks strong intensity indicate that the particles are either nanoscale in size or extremely crystalline. Interfacial bonding allows the compressing polymeric matrix to compress, making this possible.

The observed shift and change in crystallinity unequivocally demonstrate that pure n-HAp and SA and drug are bonded. Summarizing the spectra we say that HA is successfully inserted into the polymer matrix.

The polymer sodium alginate is amorphous that is why peaks are not identified using XRD. However, presence of peaks of HA confirms its crystallinity and that our prepared composites have successfully inserted HA in them.

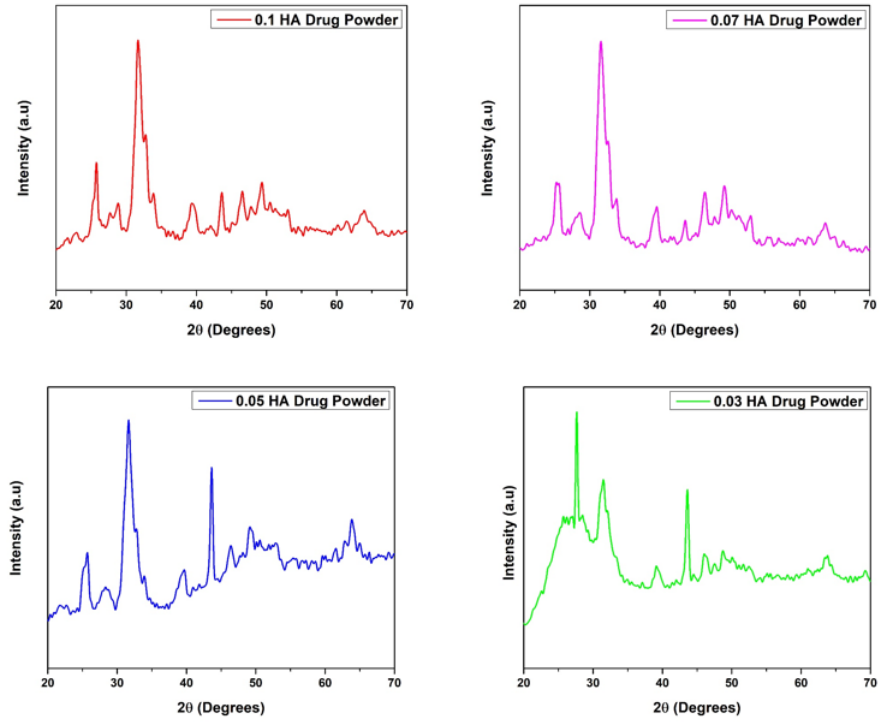


Figure 5.8: XRD Analysis of HA-Drug powder with different drug ratios

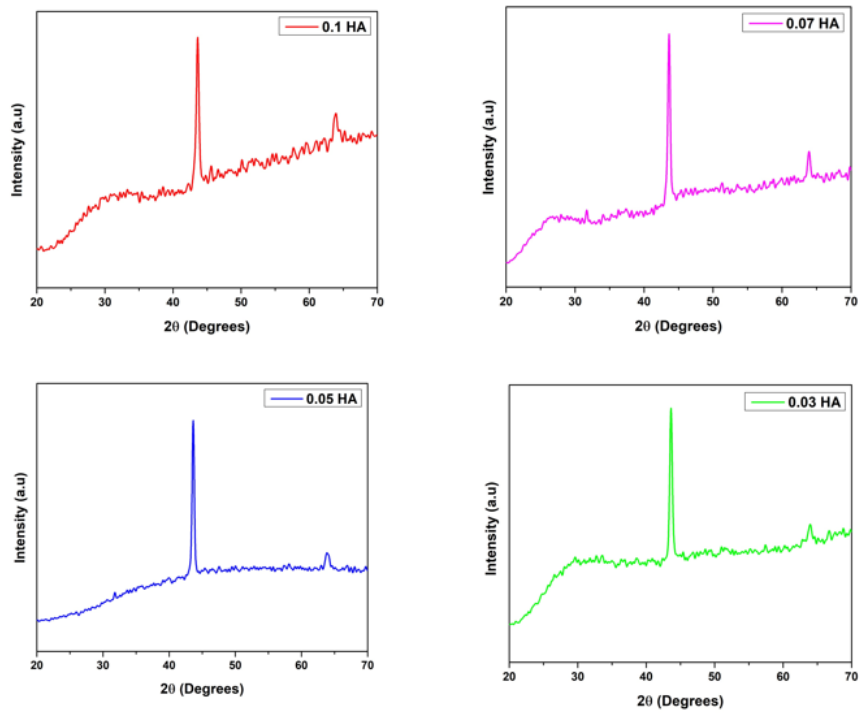


Figure 5.9: XRD Analysis of Hydroxyapatite-Alginate nanocomposite beads loaded with Drug.

5.2.3 XRD Analysis of Whitlockite-Drug Powder

The typical WH peaks at 22.0° , 25.9° , 28.0° , 31.2° , 32.7° , and 34.6° are displayed in the x-ray diffractograms of four samples. These peaks match completely with JCPDS (01-070-2064 and 00-042-0578) and the literature. Hkl (024), (1010), (214), (2010), (128), and (220) that confirms the formation of WH crystals in figure 5.7.

Also, ciprofloxacin is an organic compound belonging to the fluoroquinolone class of antibiotics so like most of the organic compounds, ciprofloxacin did not produce well-defined diffraction peaks in XRD due to its non-crystalline or amorphous nature.

However, peaks around 2 theta values of 19.22° , 26.39° and 29.16° confirms that drug has been loaded into the whitlockite matrix.

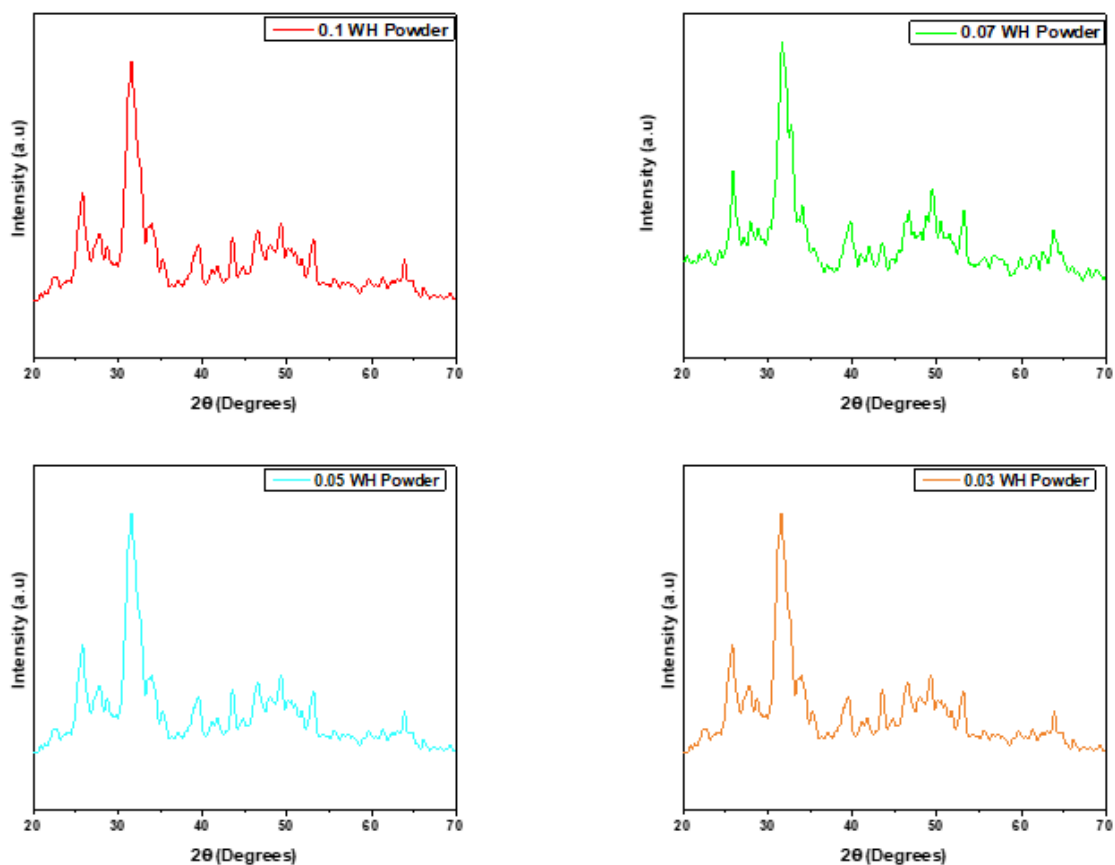


Figure 5.10: XRD Analysis of WH-Drug powder with different drug ratios

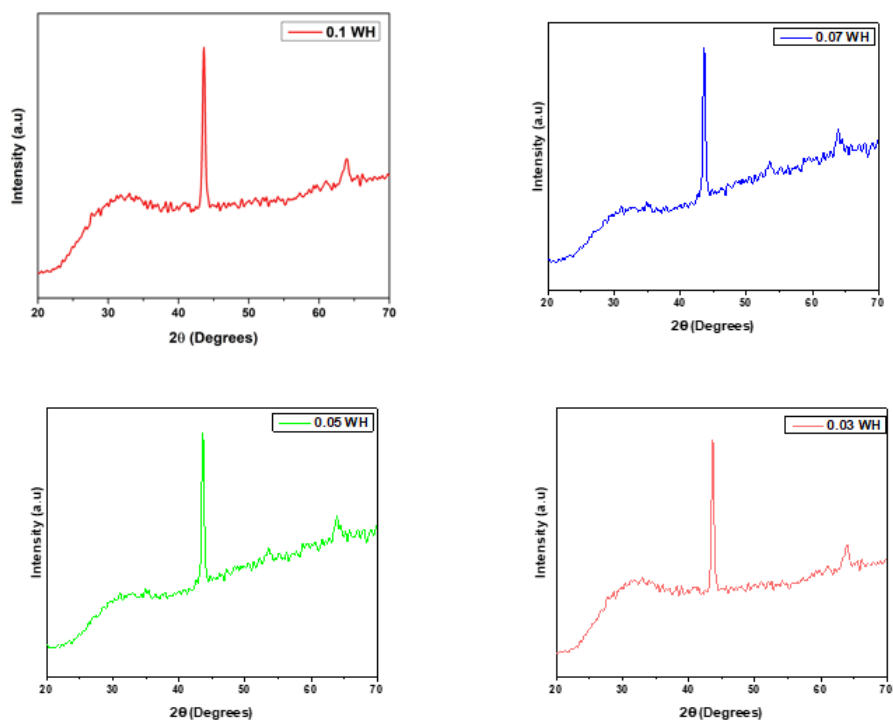


Figure 5.11: XRD Analysis of HA-Alginate nanocomposite beads loaded with different drug ratios

5.2.4 XRD of Whitlockite-Alginate nanocomposite beads loaded with Drug

The presence of WH crystals was demonstrated by the XRD pattern. The theta values around 25.8° , 31.6° , 32.1° , 39.6° , 46.8° , 49.4° these peaks correspond to the crystal structure of whitlockite and are indicative of its presence in our samples in figure 5.8. All the samples had whitlockite, drug and alginate coating. The presence of peaks of drug and whitlockite confirm that drug has been loaded into the samples. When analyzing the samples the mixtures containing both whitlockite and sodium alginate, the diffraction pattern obtained was a combination of the peaks from both substances. The sharp, well-defined peaks from whitlockite dominated the XRD pattern, while the peaks from sodium alginate were less intense or diffused. But it confirmed that polymer was evenly distributed in our samples. So we can conclude that our whitlockite nanoparticles formed chemical bonds with sodium alginate through functional groups present on their surfaces via hydrogen bonding, electrostatic interactions, and covalent bonding, which contributed to

the stability and strength of the nanocomposite which contributes a lot in drug delivery application.

5.3 Raman Analysis

The Raman analysis was used to identify the chemical composition of the samples and to study their molecular structures. We carried out Raman Analysis for all the powdered samples of hydroxyapatite and whitlockite having different drug ratios.

5.3.1 Raman Analysis of Hydroxyapatite-Drug Powder

Typical Raman peaks observed in the spectrum of hydroxyapatite seen in figure 5.9 were the phosphate stretching vibrations were the most prominent features in the Raman spectrum of hydroxyapatite. All Calcium phosphates show peaks in 950 to 960 cm^{-1} region, HA phosphate ion peak is sharp. These peaks typically were seen around 900 cm^{-1} and 1200 cm^{-1} region of spectra. The main phosphate stretching modes were around 960 cm^{-1} and 1025 cm^{-1} . Hydroxyl stretching modes:

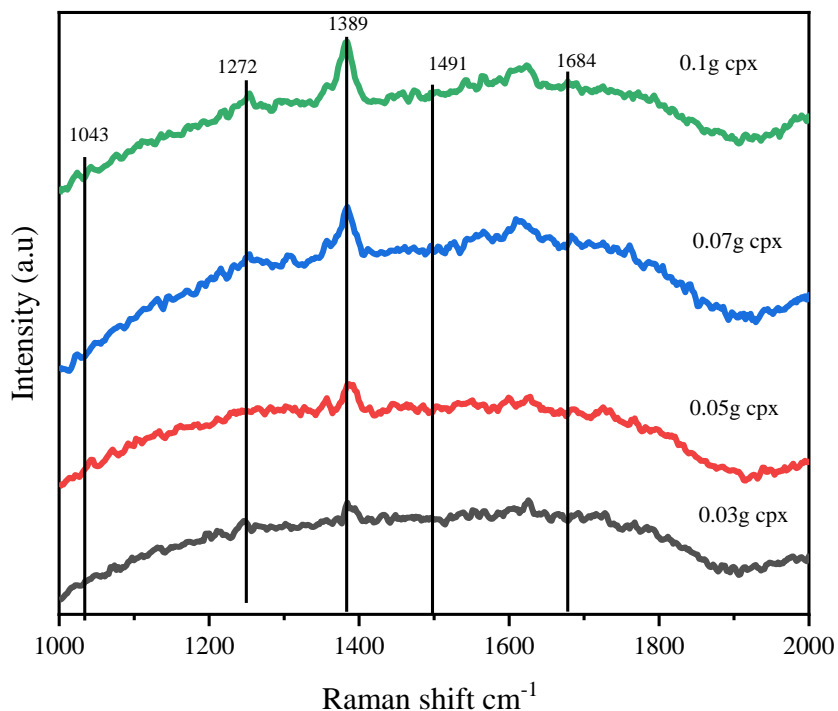


Figure 5.12: Raman Analysis of Hydroxyapatite-Drug Powder with different drug ratios

Hydroxyapatite contains hydroxyl groups, which exhibit stretching vibrations. These peaks are typically observed around 3100 cm^{-1} to 3600 cm^{-1} . The main carbonate peak is typically observed around 1070 cm^{-1} . However, in case of Ciprofloxacin the peaks around the region 1268 cm^{-1} , 1389 cm^{-1} and 1480 cm^{-1} confirmed the presence of drug in our sample. The results clearly prove that the drug has been loaded into our ceramic material.

5.3.2 Raman Analysis of Whitlockite-Drug Powder

Raman Analysis of 4 samples of Whitlockite Drug powder was carried out. The 4 samples were loaded with drug ciprofloxacin in ascending to descending order in terms of drug loading capacity shown in figure 5.10. The sample with the highest drug content i.e. 0.1g cpx showed prominent peaks. However, the one with the least drug content 0.03g of cpx showed less sharp peaks.

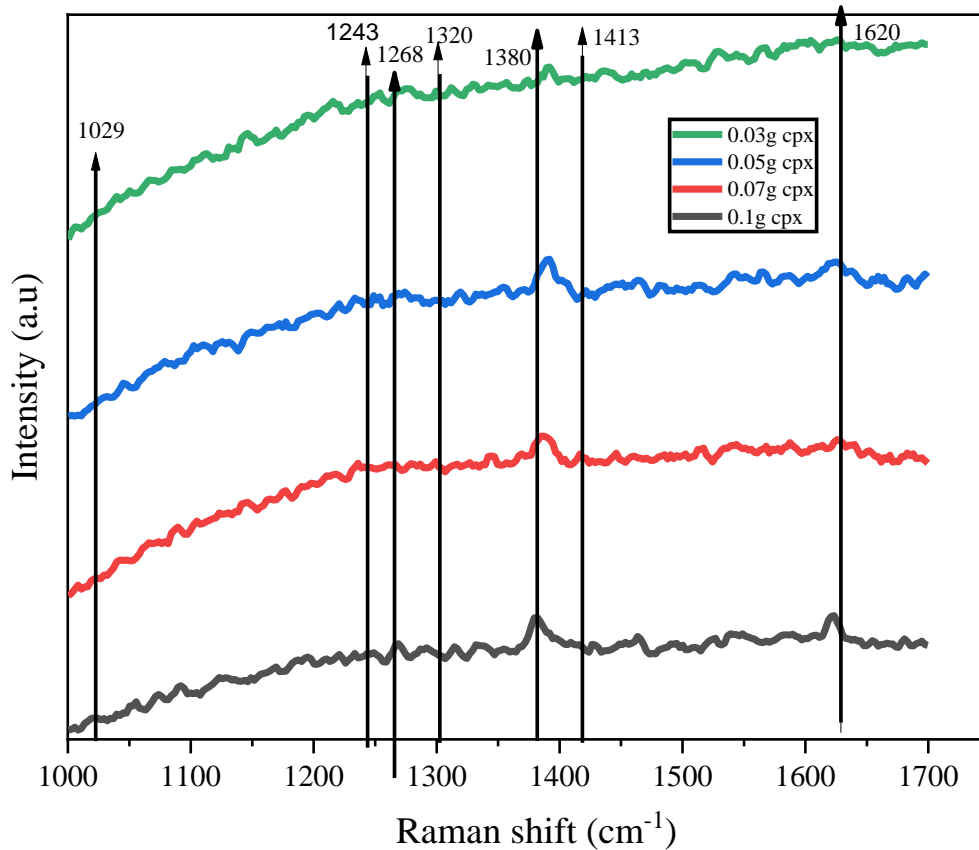


Figure 5.13: Raman Analysis of Whitlockite-Drug powder with different drug ratios

But it was confirmed from the literature that all the required peaks were present in the spectra which confirmed that our sample was clearly loaded with the drug content in different ratios. Indicating the peaks we observed that the peaks around 586 cm^{-1} , 432 cm^{-1} , 962 cm^{-1} confirm the presence of whitlockite.

The prominent peak of phosphate ion present around region 1029 cm^{-1} confirmed that our samples are pure whitlockite. Then the peaks around region 1268 cm^{-1} , 1380 cm^{-1} , 1480 cm^{-1} and 1620 cm^{-1} confirm that samples are loaded with drug ciprofloxacin as well. The samples are labelled according to the drug ratios. Hence it was proved that band intensities increase with increasing the drug loading percentages.

5.4 Scanning Electron Microscopy (SEM) of Nano composite Beads

Scanning Electron Microscopy SEM of the nanocomposite beads was done to analyze the surface and cross sectional morphology of the samples. The SEM images of all the compositions of Hydroxyapatite and Whitlockite based nanocomposite beads with different drug ratios are shown below.

5.4.1 SEM Analysis of Hydroxyapatite-Alginate beads loaded with drug

SEM analysis of nanocomposite bead samples was carried out to observe the effect of crosslinker (SA), Hydroxyapatite (HA) and antibiotic drug Ciprofloxacin on the morphology of composites. At X1000 magnification, the surface is visualized to be smooth which is due to the presence of crosslinker.

The sodium alginate induced chemical cross linking and leading to decrease in surface roughness. According to literature smoothening of cross sectional region of beads indicate increase in mechanical stiffness due to crosslinking which promotes interfiber bonding and leading to closer, denser and smoother structures.

Sample 0.1g with high drug content showed bridges which means drug and ceramic are crosslinked with the sodium alginate. Sample with drug 0.07g shows agglomeration in cross sectional region.

These points serve as points for cell adhesion. This can be a benefit in biomedical purpose. However the SA polymer surface completely encloses the n-HAp particles, preventing them from being distinguished individually and forming a cohesive composite structure.

Strong hydrogen bonding and electrostatic forces between the Ca^{2+} of HAp and the COO^- of SA are the origin of this composite structure. SEM analysis identified the composite development amongst n-HAp and SA.

5.4.2 SEM Analysis of Whitlockite-Alginate beads loaded with drug

SEM Analysis of cross-sectional region of whitlockite-alginate loaded with drug particles indicate that whitlockite has been successfully embedded into the polymer matrix. Cross linking chains are clearly seen in the images. This shows that polymer and whitlockite along with the drug were bonded via intermolecular chains.

The samples showed blocks which indicate that the samples have been cross linked. Roughness is observed in the cross-sectional view of the samples and it is confirmed from the literature that roughness is desirable for drug release and ingrowth of cellular interaction.

The voids or empty spaces seen in some SEM images is due to the fact that water molecules have been evaporated from the surface of beads creating empty spaces. This also leads to surface roughness.

These findings closely align with the documented body of literature. Because of agglomeration, the filler is not equally dispersed into the polymer matrix at greater concentrations, as demonstrated by the current situation where the addition of CaPs enhanced surface roughness.

The composite's cross-sectional photos display the blend's dense surface, but the filler's addition has left a porous surface visible. For the purpose of regenerating bone tissue, this porous network is perfect.

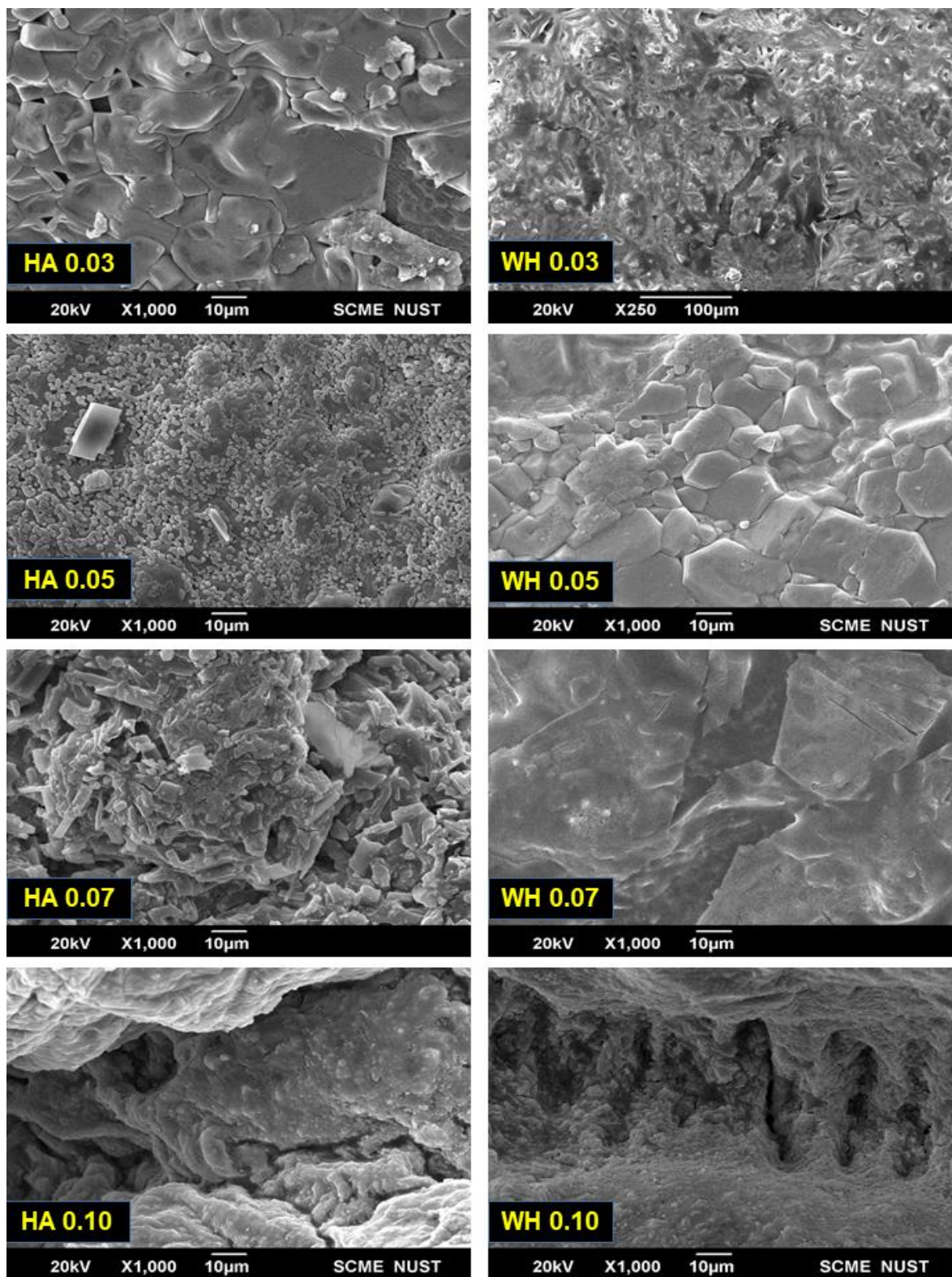


Figure 5.14: SEM analysis of HA-Alginate and WH-Alginate nanocomposite beads loaded with different drug ratios

5.5 Swelling behavior of HA-Alginate beads loaded with drug

Swelling behavior is important parameter for a drug delivery vehicle because it influences regulated drug delivery behavior. Swelling test of nanocomposite beads was conducted as described in chapter 4. The readings were recorded, and percentage swelling was calculated using the following equation 5.1:

$$\% \text{ swelling} = (W_f - W_i) / W_i * 100 \quad (5.1)$$

Final results are plotted in graph in figure which have indicated following results:

In order to analyze the swelling behaviour, the weight of the samples was determined over time in order to evaluate the swelling behaviour, as illustrated in Figure. Beads made of nanocomposite materials should absorb water or media appropriately. A nanocomposite bead's ability to absorb water and nutrients can be inferred by swelling studies.

To find out if HA affects nanocomposites swelling, the amount of swelling was tested in a buffer with a pH of 7.4. Hydrophilic hydroxyl groups and the anionic sulphate groups and their repulsion force, and osmotic pressure inside beads caused swelling to increase.

Our results showed that the samples behaved similarly, reaching swelling equilibrium regardless of the HA percentage after 24 hours. The swelling method was typically used to confirm drug release from alginate matrices as shown in figure 5.12.

It showed how quickly and easily a liquid entered a gel matrix, which had a big impact on how drugs release. Alginate HA beads loaded with drugs swelled quickly in 24 hours at pH 7.4 because the sodium alginate's carboxylic group broke down.

More transport of water molecules and hence more swelling ratio. The beads with greater amount of drug (0.1g cpx) showed more swelling percentage besides the one which has least drug content (0.03g cpx).

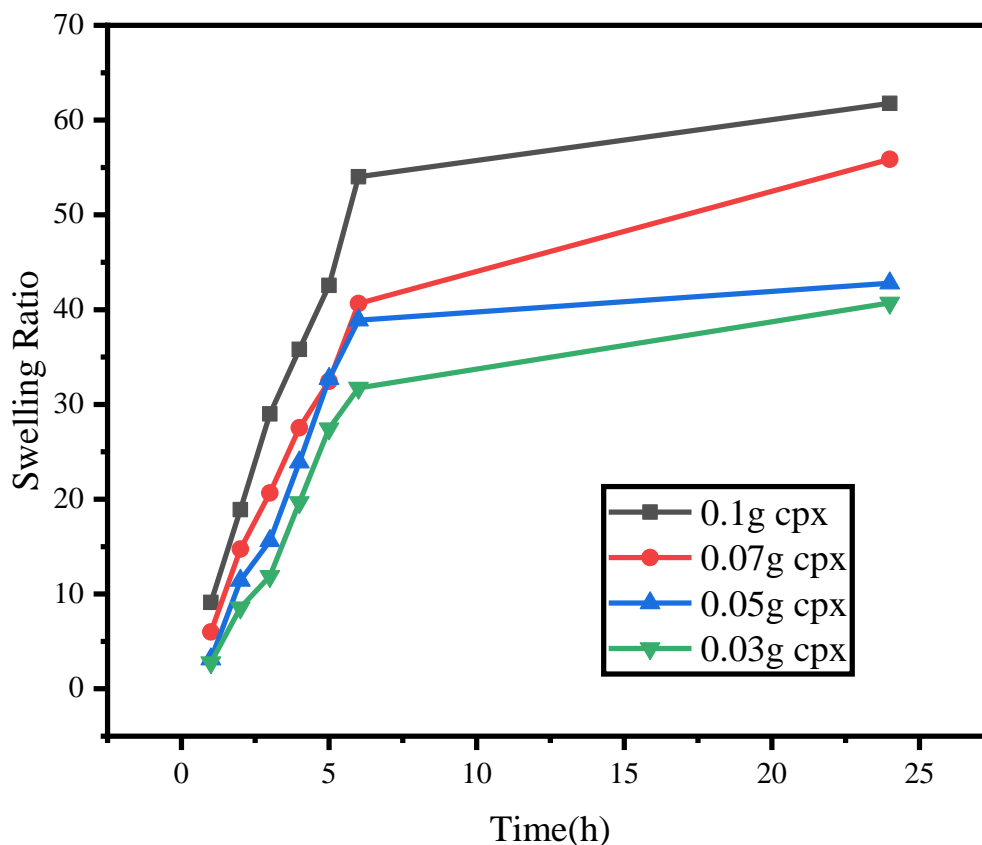


Figure 5.15: Swelling Behaviour of HA-Alginate nanocomposite beads loaded with different drug ratios

5.6 Swelling behavior of WH-Alginate beads loaded with drug

Swelling behavior is an intrinsic behavior that helps to study more about drug delivery behavior of composites. Swelling test of nanocomposite beads was conducted as described in chapter 4. The readings were recorded and amount of swelling in percentage was calculated using the following equation 5.2:

$$\% \text{ Swelling} = \frac{w_f - w_i}{w_i} * 100 \quad (5.2)$$

Final results are plotted in graph in figure which have indicated following results:

The results suggested that polymeric chains were securely anchored by nanoparticles in their local area, which ultimately resulted in increased network density. In addition to improving the integrity of the nanocomposites, this cross-linked networking and hydrophilic character holds an important role in the expansion of the swelling ratio. The fact that sodium alginate is hydrophilic may be the only explanation for the rise in water absorption with alginate concentration. In the first twenty-four hours, there was a noticeable shift, and then equilibrium was reached. The osmotic pressure-driven movement of water molecules into the polymeric matrix was responsible for the swelling ratio rise that occurs during the first three hours. These beads started to absorb water when placed in phosphate buffer solution having a pH of 7.4.

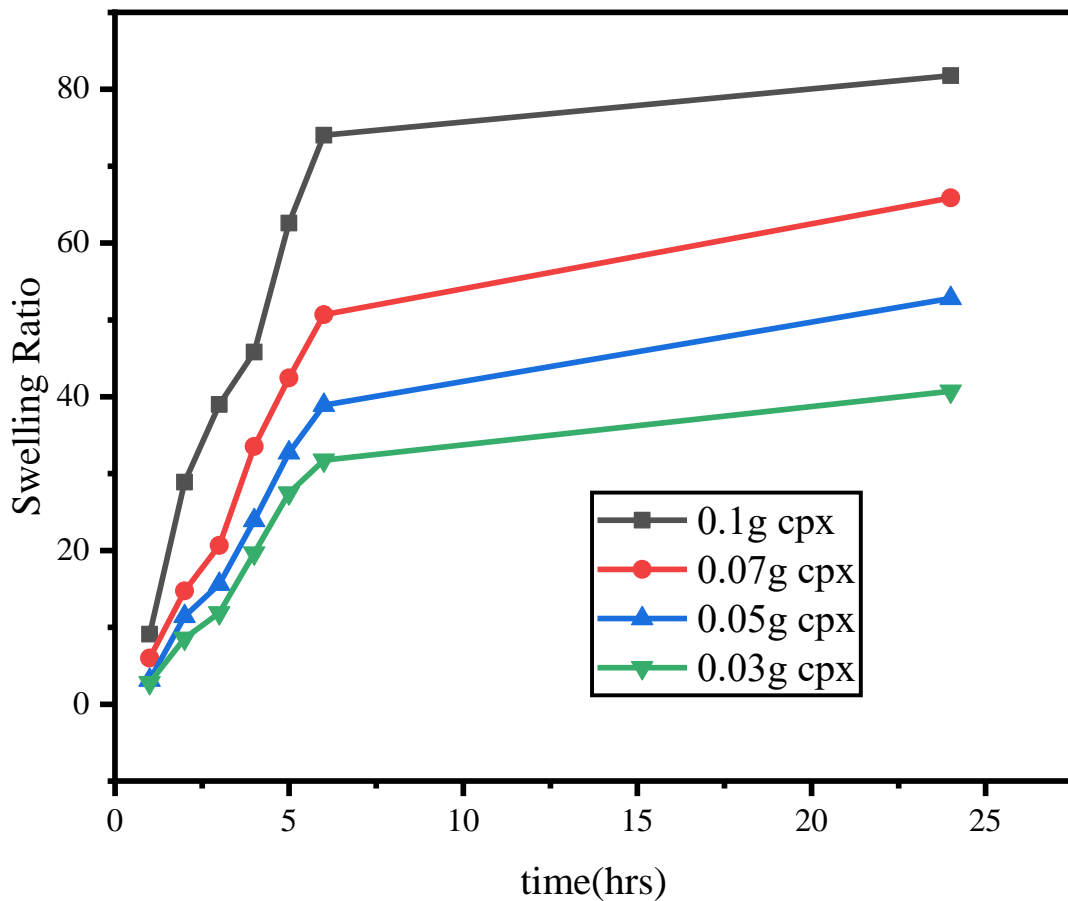


Figure 5.16: Swelling Behaviour of WH-Alginate nanocomposite beads loaded with different drug ratios

Sample -1(0.1g CPX) of Whitlockite Nano composite which had the greatest amount of drug loaded in it showed the highest swelling ratio followed by Sample- 2(0.07g CPX). Likewise, Sample-3(0.05g CPX) and sample-4(0.03g CPX) which had the lowest amount of drug content showed the decreased swelling behavior. Increase in swelling of the cross-linked polyelectrolytes (like SA) in this work were mostly ascribed to phenomenon of the charged polymer chain's hydrophilicity and electrostatic repulsion as demonstrated by WH-based nanocomposite beads. The lowered swelling ratio in start is caused by a drop in the relative content of SA and an increase in WH microparticles in the nanocomposite beads as the drug content decreased. Large-scale segmental motion causes the beads to swell, which eventually increases the space between the polymer chains.

The increased swelling ratio (Sample 1) with the highest drug content 0.1g confirmed that the SA/WH nanocomposite beads were loosely crosslinked, which facilitated more penetration of water into the composite beads, and hence made them swell more with a mark up to 80 percent.

5.7 Drug Delivery Analysis of HA-Alginate beads loaded with drug

Drug delivery is becoming more and more important for the cure of human diseases, bone implantation, and bone tissue regeneration. In clinical practice, the addition of medications to bioceramic matrices may prove to be quite intriguing. These days, it is typical for an orthopaedic surgeon who does bone repair to use biomaterials in either dense or porous form with predetermined shapes. These delivery methods offer viable substitutes for parenteral medication administration, especially in the case of peptide and protein therapies. Numerous drug delivery strategies have been developed and are being researched for this reason.

In this report ciprofloxacin loaded hydroxyapatite - alginate beads were studied as the drug delivery system and we studied the drug release trend. Concentration of HA mineral and polymer were kept constant and the drug concentration was changed.

At 37 °C and a pH of 7.4, the drug release behaviour of the Ciprofloxacin loaded on nHA-alginate Nano composite was monitored for a full day. As can be shown, the

release of the surface-bounded medication from the Nano composite is responsible for the first two hours of the observed burst release of ciprofloxacin. A continuous release of the medication was seen for the course of the 24-hour incubation period following the first burst release. The drug was slowly released over a longer period of time as a result of the medium's alginate disintegrating and the drug diffusing from the composite matrix. The consistent dispersion of the medication throughout the composite matrix was also demonstrated by this persistent release behaviour. This shows that the drug is released in a very slow and sustained way. The amount of released drug in 24 hours of time is well explained as 100% of drug was released in 24 hours. Alginate encapsulation prolonged the drug release. This work highlights the significance of choosing appropriate materials to optimise drug release kinetics for increased efficacy in medical applications and validates the role that material qualities play in drug delivery systems.

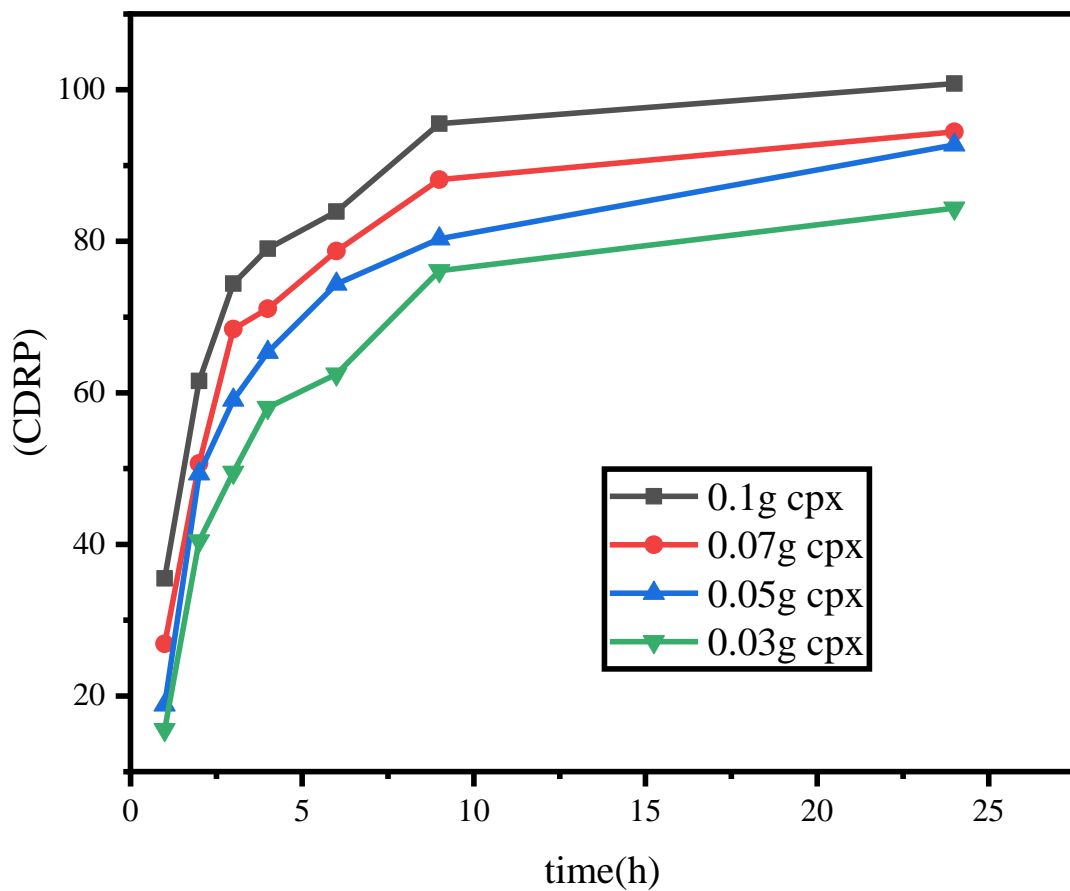


Figure 5.17: Drug Delivery Analysis of HA-Alginate nanocomposite beads loaded with different drug ratios

5.8 Drug Delivery Analysis of WH-Alginate beads loaded with drug

In this study, we carried out drug release tests on Whitlockite-Alginate nanocomposite beads loaded with drug ciprofloxacin. The drug release was estimated over time using the technique UV spectroscopy. The graph below shows the amount of drug released in percentage from the samples at different time intervals revealing distinct drug release profiles.

The drug release percentage at a given time (t) was calculated using the following equation 5.3:

$$\text{Percentage of Drug Loading} = \frac{A-B}{A} * 100 \quad (5.3)$$

Where A and B represent the initial and final drug concentration.

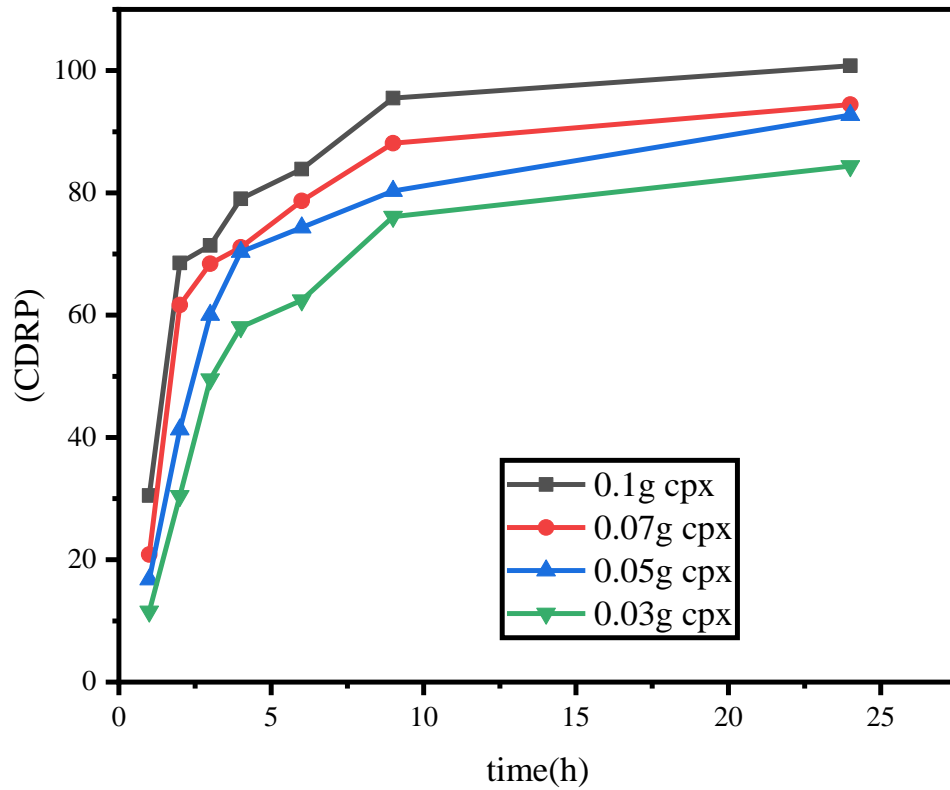


Figure 5.18: Drug Delivery Analysis of WH-Alginate nanocomposite beads loaded with different drug ratios

The results demonstrate that with the increase in drug concentration drug release rate was also increased. But it is seen that with the time there was a gradual increase in drug release rate rate. Peaks are clearly seen in the graph. After 1st reading which was conducted after 1 hour it was observed that a slow drug release was seen. After 12 hours almost 80% of drug was released. There was no burst release observed, there was a sustained drug release seen which is an advantage for the biomedical application. After 12-24hrs 100% drug was released. However, it was studied in literature that ciprofloxacin has a serum half-life of roughly 4-6 hours. It is promptly and thoroughly absorbed after oral intake of single doses of 250 mg, 500 mg, and 750 mg tablets, primarily from the small intestine. After a time period of 2 hours, 50–70% of an administered dose is eliminated as unmetabolized medication in the urine. Ten percent more is eliminated as metabolites in the urine. Almost entire urine excretion occurs within 24 hours of treatment.

CHAPTER 6: CONCLUSIONS AND FUTURE RECOMMENDATION

6.1 Conclusion

Nanocomposite beads of Hydroxyapatite and Whitlockite containing different concentrations of drug i.e. Ciprofloxacin were efficiently synthesized by utilizing wet chemical precipitation method. The drug was loaded onto the ceramic particles before the formation of beads. The ceramic and drug powder were stirred in sodium alginate to form the paste. However, the presence of sodium alginate in the mixture did not bring any change to the chemical composition of the ceramic NPs but prolonged the release of drug. We drew a comparison between the composite beads of HA and WH NPs.

The FT-IR Analysis, XRD and Raman Analysis confirmed that the drug was successfully loaded onto the ceramic particles. The SEM Analysis of the composite beads was done to determine the cross-sectional regions and it confirmed the cross linking between the polymer and the NPs. Swelling behaviour of the nanocomposites was studied for a period of 24Hrs while keeping the beads soaked in PBS solution at pH 7.8.

The swelling increased with the passage of time it is because that the drug is itself hydrophilic in nature and absorbs water. The most important application regarding bone tissue regeneration i.e. Drug Release studies were done to observe the slow and sustained release of the drug from the composite beads.

The study on drug release was done for a period of 24Hrs and it was seen that sodium alginate encapsulation played an important role in the slow and sustained release of the drug from the beads which is important for bone tissue regeneration in body.

After complete examination and investigation following conclusions were made based on our experimentation and analysis:

We expect that the HA and WH nanocomposite beads loaded with drug will be useful for the treatment of bone defects as both the ceramic NPs are identical materials with human bone minerals.

We also expect that this research could contribute to studies for developing more bone mimetic materials and develop an understanding of the structure and chemical compositions of bone components with those minerals.

Also, in future further studies should be done on the chemistry of interaction between various drugs, biomaterials and different polymers for a better justification regarding biomedical engineering.

6.2 Future Work and Recommendation

As Hydroxyapatite and Whitlockite have shown potential in bone regeneration and wound healing therefore, they hold significant importance in various fields. The potential future directions can be Biomedical Applications, Orthopedic Implants, Drug Delivery systems, Bioactive Coatings, Regenerative medicines, Dental Materials, Biomineralization studies, Environmental Remediation and Nanotechnology.

Hence, Investigating the synergistic effects of combining hydroxyapatite and whitlockite with other biomaterials, such as polymers or nanoparticles, could lead to the development of multifunctional materials with enhanced properties for biomedical applications. Overall, future work related to hydroxyapatite and whitlockite is likely to continue expanding their applications across diverse fields.

REFERENCES

- [1] G. L. Hornyak, H. F. Tibbals, J. Dutta, and J. J. Moore, *Introduction to nanoscience and nanotechnology*. CRC press, 2008.
- [2] P. Singh, M. J. Gonzalez, and M. J. D. d. r. Manchester, "Viruses and their uses in nanotechnology," vol. 67, no. 1, pp. 23-41, 2006.
- [3] J. J. S. D. Altmann, "Military uses of nanotechnology: perspectives and concerns," vol. 35, no. 1, pp. 61-79, 2004.
- [4] S. Sim and N. K. J. B. r. Wong, "Nanotechnology and its use in imaging and drug delivery," vol. 14, no. 5, pp. 1-9, 2021.
- [5] A. J. Salinas and M. J. Z. f. a. u. a. C. Vallet-Regí, "Evolution of ceramics with medical applications," vol. 633, no. 11-12, pp. 1762-1773, 2007.
- [6] S. V. J. B. Dorozhkin, "Bioceramics of calcium orthophosphates," vol. 31, no. 7, pp. 1465-1485, 2010.
- [7] Y. Zare, I. J. M. S. Shabani, and E. C, "Polymer/metal nanocomposites for biomedical applications," vol. 60, pp. 195-203, 2016.
- [8] G. D. Venkatasubbu, S. Ramasamy, V. Ramakrishnan, and J. J. J. o. b. n. Kumar, "Hydroxyapatite-alginate nanocomposite as drug delivery matrix for sustained release of ciprofloxacin," vol. 7, no. 6, pp. 759-767, 2011.
- [9] A. K. J. I. J. o. C. R. Nayak, "Hydroxyapatite synthesis methodologies: an overview," vol. 2, no. 2, pp. 903-907, 2010.
- [10] V. Orlovskii, V. Komlev, and S. J. I. m. Barinov, "Hydroxyapatite and hydroxyapatite-based ceramics," vol. 38, pp. 973-984, 2002.
- [11] K. Fox, P. A. Tran, and N. J. C. Tran, "Recent advances in research applications of nanophase hydroxyapatite," vol. 13, no. 10, pp. 2495-2506, 2012.

- [12] H. J. B. Oonishi, "Orthopaedic applications of hydroxyapatite," vol. 12, no. 2, pp. 171-178, 1991.
- [13] V. S. Kattimani, S. Kondaka, K. P. J. B. Lingamaneni, and T. R. Insights, "Hydroxyapatite—Past, present, and future in bone regeneration," vol. 7, p. BTRI. S36138, 2016.
- [14] M. Jarcho, R. Salsbury, M. Thomas, and R. J. J. o. M. S. Doremus, "Synthesis and fabrication of β -tricalcium phosphate (whitlockite) ceramics for potential prosthetic applications," vol. 14, pp. 142-150, 1979.
- [15] C. J. A. M. J. o. E. Frondel and P. Materials, "Whitlockite: a new calcium phosphate, $\text{Ca}_3(\text{PO}_4)_2$," vol. 26, no. 3, pp. 145-152, 1941.
- [16] F. A. J. A. B. Shah, "Magnesium whitlockite—omnipresent in pathological mineralisation of soft tissues but not a significant inorganic constituent of bone," vol. 125, pp. 72-82, 2021.
- [17] H. Hecht and S. J. B. Srebnik, "Structural characterization of sodium alginate and calcium alginate," vol. 17, no. 6, pp. 2160-2167, 2016.
- [18] H. L. Walker and W. J. J. W. s. Connick, "Sodium alginate for production and formulation of mycoherbicides," vol. 31, no. 3, pp. 333-338, 1983.
- [19] S. Thakur, B. Sharma, A. Verma, J. Chaudhary, S. Tamulevicius, and V. K. J. J. o. c. p. Thakur, "Recent progress in sodium alginate based sustainable hydrogels for environmental applications," vol. 198, pp. 143-159, 2018.
- [20] B. Jadach, W. Świetlik, and A. J. J. o. P. S. Froelich, "Sodium alginate as a pharmaceutical excipient: novel applications of a well-known polymer," 2022.
- [21] M. U. A. Khan, S. I. Abd Razak, S. Rehman, A. Hasan, S. Qureshi, and G. M. J. I. j. o. b. m. Stojanović, "Bioactive scaffold (sodium alginate)-g-(nHAp@ SiO_2 @ GO) for bone tissue engineering," vol. 222, pp. 462-472, 2022.

- [22] R. Greenberg *et al.*, "Treatment of bone, joint, and soft-tissue infections with oral ciprofloxacin," vol. 31, no. 2, pp. 151-155, 1987.
- [23] T. Thai, B. H. Salisbury, and P. M. Zito, "Ciprofloxacin," in *StatPearls [Internet]*: StatPearls Publishing, 2021.
- [24] P. J. J. o. a. c. Ball, "Ciprofloxacin: an overview of adverse experiences," vol. 18, no. Supplement_D, pp. 187-193, 1986.
- [25] C. Castro *et al.*, "Ciprofloxacin implants for bone infection. In vitro–in vivo characterization," vol. 93, no. 3, pp. 341-354, 2003.
- [26] S. Bose and S. J. A. b. Tarafder, "Calcium phosphate ceramic systems in growth factor and drug delivery for bone tissue engineering: a review," vol. 8, no. 4, pp. 1401-1421, 2012.
- [27] X. Liu and P. X. J. A. o. b. e. Ma, "Polymeric scaffolds for bone tissue engineering," vol. 32, pp. 477-486, 2004.
- [28] B. Leukers *et al.*, "Hydroxyapatite scaffolds for bone tissue engineering made by 3D printing," vol. 16, no. 12, pp. 1121-1124, 2005.
- [29] S. R. Motamedian, S. Hosseinpour, M. G. Ahsaie, and A. J. W. j. o. s. c. Khojasteh, "Smart scaffolds in bone tissue engineering: A systematic review of literature," vol. 7, no. 3, p. 657, 2015.
- [30] X. Liu, Y. Mou, S. Wu, and H. C. J. A. s. s. Man, "Synthesis of silver-incorporated hydroxyapatite nanocomposites for antimicrobial implant coatings," vol. 273, pp. 748-757, 2013.
- [31] C. C. J. I. J. o. E. R. Okpala and Development, "Nanocomposites—an overview," vol. 8, no. 11, pp. 17-23, 2013.
- [32] A. Lagashetty and A. J. R. Venkataraman, "Polymer nanocomposites," vol. 10, pp. 49-57, 2005.

- [33] R. A. Hule and D. J. J. M. b. Pochan, "Polymer nanocomposites for biomedical applications," vol. 32, no. 4, pp. 354-358, 2007.
- [34] M. A. Maghsoudlou, E. Nassireslami, S. Saber-Samandari, and A. J. A. J. o. M. B. Khandan, "Bone regeneration using bio-nanocomposite tissue reinforced with bioactive nanoparticles for femoral defect applications in medicine," vol. 12, no. 2, p. 68, 2020.
- [35] A. R. Boccaccini *et al.*, "Polymer/bioactive glass nanocomposites for biomedical applications: a review," vol. 70, no. 13, pp. 1764-1776, 2010.
- [36] S. Noreen *et al.*, "Multifunctional mesoporous silica-based nanocomposites: Synthesis and biomedical applications," vol. 285, p. 126132, 2022.
- [37] L. Zhang, M. Liu, Z. Fang, and Q. J. C. C. R. Ju, "Synthesis and biomedical application of nanocomposites integrating metal-organic frameworks with upconversion nanoparticles," vol. 468, p. 214641, 2022.
- [38] A. Jayalekshmi, S. P. Victor, C. P. J. C. Sharma, and S. B. Biointerfaces, "Magnetic and degradable polymer/bioactive glass composite nanoparticles for biomedical applications," vol. 101, pp. 196-204, 2013.
- [39] M. Mozafari *et al.*, "Development of 3D bioactive nanocomposite scaffolds made from gelatin and nano bioactive glass for biomedical applications," vol. 19, no. 2, p. 096369351001900204, 2010.
- [40] R. Jayakumar, D. Menon, K. Manzoor, S. V. Nair, and H. J. C. p. Tamura, "Biomedical applications of chitin and chitosan based nanomaterials—A short review," vol. 82, no. 2, pp. 227-232, 2010.
- [41] A. K. Gaharwar, N. A. Peppas, A. J. B. Khademhosseini, and bioengineering, "Nanocomposite hydrogels for biomedical applications," vol. 111, no. 3, pp. 441-453, 2014.

- [42] S. Huang *et al.*, "Nanocomposite hydrogels for biomedical applications," vol. 7, no. 3, p. e10315, 2022.
- [43] K. Phogat, S. B. Ghosh, and S. J. J. o. A. P. S. Bandyopadhyay-Ghosh, "Recent advances on injectable nanocomposite hydrogels towards bone tissue rehabilitation," vol. 140, no. 4, p. e53362, 2023.
- [44] M. Amiri, P. Khazaeli, A. Salehabadi, M. J. A. i. c. Salavati-Niasari, and i. science, "Hydrogel beads-based nanocomposites in novel drug delivery platforms: Recent trends and developments," vol. 288, p. 102316, 2021.
- [45] W. M. Kedir, G. F. Abdi, M. M. Goro, and L. D. J. H. Tolesa, "Pharmaceutical and drug delivery applications of chitosan biopolymer and its modified nanocomposite: A review," p. e10196, 2022.
- [46] L. Sukhodub *et al.*, "Antibacterial and physical characteristics of silver-loaded hydroxyapatite/alginate composites," vol. 3, no. 4, p. 045010, 2021.
- [47] S. Das *et al.*, "Alginate–montmorillonite composite systems as sustained drug delivery carriers," in *Alginates in Drug Delivery*: Elsevier, 2020, pp. 187-201.
- [48] K. Sangeetha and E. J. J. o. B. Girija, "Effect of alginate on hydroxyapatite/gelatin nanocomposites for orthopedic applications," vol. 10, no. 4, pp. 257-266, 2016.
- [49] A. K. Nayak, M. S. Hasnain, S. S. Nanda, and D. K. J. C. P. D. Yi, "Hydroxyapatite-alginate based matrices for drug delivery," vol. 25, no. 31, pp. 3406-3416, 2019.
- [50] J. Zhang, Q. Wang, and A. J. A. B. Wang, "In situ generation of sodium alginate/hydroxyapatite nanocomposite beads as drug-controlled release matrices," vol. 6, no. 2, pp. 445-454, 2010.
- [51] L. Fan, J. Zhang, and A. J. J. o. M. C. B. Wang, "In situ generation of sodium alginate/hydroxyapatite/halloysite nanotubes nanocomposite hydrogel beads as drug-controlled release matrices," vol. 1, no. 45, pp. 6261-6270, 2013.

- [52] L. F. Sukhodub, L. B. Sukhodub, O. Litsis, Y. J. M. C. Prylutsky, and Physics, "Synthesis and characterization of hydroxyapatite-alginate nanostructured composites for the controlled drug release," vol. 217, pp. 228-234, 2018.
- [53] C. Onoyima, F. Okibe, Q. J. N. J. o. P. Sholadoye, and A. S. Research, "Kinetics and mechanisms of doxorubicin release from hydroxyapatite-sodium alginate nanocomposite," vol. 9, no. 3, pp. 7-13, 2020.
- [54] M. Hafezi, M. Abbasi-shahnib, A. Zamanian, and S. J. J. o. C. P. R. Hesaraki, "Preparation and characterization of whitlockite-merwinite nanocomposite," vol. 14, no. 1, pp. 96-99, 2013.
- [55] R. Yegappan, V. Selvaprithviraj, S. Amirthalingam, A. Mohandas, N. S. Hwang, and R. J. I. j. o. b. m. Jayakumar, "Injectable angiogenic and osteogenic carrageenan nanocomposite hydrogel for bone tissue engineering," vol. 122, pp. 320-328, 2019.
- [56] F. Nazir, L. Abbas, and M. J. A. N. Iqbal, "A comparative insight into the mechanical properties, antibacterial potential, and cytotoxicity profile of nano-hydroxyapatite and nano-whitlockite-incorporated poly-L-lactic acid for bone tissue engineering," vol. 12, pp. 47-68, 2022.
- [57] S. Amirthalingam, A. Ramesh, S. S. Lee, N. S. Hwang, and R. J. A. A. B. M. Jayakumar, "Injectable in situ shape-forming osteogenic nanocomposite hydrogel for regenerating irregular bone defects," vol. 1, no. 4, pp. 1037-1046, 2018.